

# 1 Terpenes and their oxidation products in the French Landes forest: 2 insight from Vocus PTR-TOF measurements

3 Haiyan Li<sup>1</sup>, Matthieu Riva<sup>2</sup>, Pekka Rantala<sup>1</sup>, Liine Heikkinen<sup>1</sup>, Kaspar Daellenbach<sup>1</sup>, Jordan E.  
4 Krechmer<sup>3</sup>, Pierre-Marie Flaud<sup>4,5</sup>, Douglas Worsnop<sup>3</sup>, Markku Kulmala<sup>1</sup>, Eric Villenave<sup>4,5</sup>, Emilie  
5 Perraudin<sup>4,5</sup>, Mikael Ehn<sup>1</sup>, Federico Bianchi<sup>1</sup>

6 <sup>1</sup> Institute for Atmospheric and Earth System Research / Physics, Faculty of Science, University of Helsinki, Finland

7 <sup>2</sup> Univ. Lyon, Université Claude Bernard Lyon 1, CNRS, IRCELYON, F-69626, Villeurbanne, France

8 <sup>3</sup> Aerodyne Research Inc., Billerica, Massachusetts 01821, USA

9 <sup>4</sup> Univ. Bordeaux, EPOC, UMR 5805, F-33405 Talence Cedex, France

10 <sup>5</sup> CNRS, EPOC, UMR 5805, F-33405 Talence Cedex, France

11 Correspondence: Haiyan Li ([haiyan.li@helsinki.fi](mailto:haiyan.li@helsinki.fi)) and Matthieu Riva ([matthieu.riva@ircelyon.univ-lyon1.fr](mailto:matthieu.riva@ircelyon.univ-lyon1.fr))

12 **Abstract.** The capabilities of the recently developed Vocus proton-transfer-reaction time-of-flight mass spectrometer (PTR-  
13 TOF) are reported for the first time based on ambient measurements. With the deployment of the Vocus PTR-TOF, we present  
14 an overview of the observed gas-phase (oxygenated) molecules in the French Landes forest during summertime 2018 and gain  
15 insights into the atmospheric oxidation of terpenes, which are emitted in large quantities in the atmosphere and play important  
16 roles in secondary organic aerosol production. Due to the greatly improved detection efficiency compared to conventional  
17 PTR instruments, the Vocus PTR-TOF identifies a large amount of gas-phase signals with elemental composition categories  
18 including CH, CHO, CHN, CHS, CHON, CHOS, and others. Multiple hydrocarbons are detected, with carbon numbers up to  
19 20. Particularly, we report the first direct observations of low-volatility diterpenes in the ambient air. The diurnal cycle of  
20 diterpenes is similar to that of monoterpenes and sesquiterpenes, but contrary to that of isoprene. Various types of terpene  
21 reaction products and intermediates are also characterized. Generally, the more oxidized products from terpene oxidations  
22 show a broad peak in the day due to the strong photochemical effects, while the less oxygenated products peak in the early  
23 morning and/or in the evening. To evaluate the importance of different formation pathways in terpene chemistry, the reaction  
24 rates of terpenes with main oxidants (i.e., hydroxyl radical, OH; ozone, O<sub>3</sub>; and nitrate radical, NO<sub>3</sub>) are calculated. For the  
25 less oxidized non-nitrate monoterpene oxidation products, their morning and evening peaks have contributions from both O<sub>3</sub>-  
26 and OH-initiated monoterpene oxidation. For the monoterpene-derived organic nitrates, oxidations by O<sub>3</sub>, OH, and NO<sub>3</sub>  
27 radicals all contribute to their formation, with their relative roles varying considerably over the course of the day. Through a  
28 detailed analysis of terpene chemistry, this study demonstrates the capability of the Vocus PTR-TOF in the detection of a wide  
29 range of oxidized reaction products in ambient and remote conditions, which highlights its importance in investigating  
30 atmospheric oxidation processes.

## 31 1. Introduction

32 Organic aerosol (OA) constitutes a large fraction of atmospheric particles, having significant impacts on climate change, air  
33 quality, and human health (Maria et al., 2004; IPCC, 2013; Mauderly and Chow, 2008). On a global scale, secondary OA  
34 (SOA) is the largest source of OA, formed through the oxidation of volatile organic compounds (VOCs) (Jimenez et al., 2009).  
35 Biogenic VOCs (BVOCs) are released into the atmosphere in high amounts, with an annual global budget being 760 Tg C  
36 (Sindelarova et al., 2014). On average, SOA production from biogenic precursors ranges from 2.5 to 44.5 Tg C annually, which  
37 is much larger than that from anthropogenic sources (Tsigaridis and Kanakidou, 2003). Over the past decades, a considerable  
38 amount of studies has been conducted to investigate the atmospheric chemistry of BVOCs (Kanakidou et al., 2005; Henze et  
39 al., 2006; Hatfield et al., 2011; Calfapietra et al., 2013; Jokinen et al., 2015; Ng et al., 2017). However, an incomplete

40 understanding of BVOCs characteristics and their oxidation processes in the atmosphere remains and yields large uncertainties  
41 in quantitative estimates of air quality and climate effects of atmospheric aerosols (Carslaw et al., 2013; Zhu et al., 2019).

42 Terpenes make up the main fraction of BVOCs (Guenther et al., 1995), encompassing isoprene ( $C_5H_8$ ), monoterpenes  
43 ( $C_{10}H_{16}$ ), sesquiterpenes ( $C_{15}H_{24}$ ), diterpenes ( $C_{20}H_{32}$ ) and even larger compounds. With one or more C=C double bonds in  
44 their molecular structures, terpenes are highly reactive. After entering the atmosphere, terpenes can undergo oxidative  
45 chemistry with the common atmospheric oxidants including hydroxyl radical (OH), ozone ( $O_3$ ), and nitrate radical ( $NO_3$ ).  
46 These oxidation processes generate a large variety of organic species, with volatilities ranging from gas-phase volatile species  
47 (VOC), to semi-volatile / low volatility organic compounds (SVOC and LVOC), to extremely low volatility organic  
48 compounds (ELVOC) and even ultra-low volatility organic compounds (ULVOC), which irreversibly contribute to SOA  
49 formation (Donahue et al., 2012). Due to the chemical complexity and low concentrations of BVOCs oxidation products, it  
50 remains extremely challenging to provide a comprehensive understanding of terpene chemistry in the atmosphere.

51 With a high time response and sensitivity, proton-transfer-reaction mass spectrometry (PTR-MS) has been widely  
52 used to study the emissions and chemical evolution of VOCs in the atmosphere (Yuan et al., 2017). However, due to the  
53 relatively low sensitivity, previous PTR-MS instruments were not optimized to detect low volatility compounds. For example,  
54 only a few ambient PTR-MS observations of sesquiterpenes are available (Kim et al., 2009; Jardine et al., 2011).  
55 Correspondingly, it is not surprising that ambient observations of diterpenes, which are generally considered to be non-volatile  
56 compounds, have never been reported. In addition, the existing PTR-MS is often not sensitive enough to quantify terpene  
57 oxidation products at atmospherically relevant concentrations (Yuan et al., 2017). To address these instrumental limitations,  
58 two new versions of PTR were recently developed, the PTR3 (Breitenlechner et al., 2017) and the Vocus PTR-TOF (Krechmer  
59 et al., 2018), both coupled with a time of flight (TOF) mass analyzer. With the enhanced sensitivities by a factor of  $\sim 10$   
60 (Holzinger et al., 2019), these instruments are capable of detecting broader spectrum of VOCs, where the detection of low-  
61 volatility VOCs is significantly improved compared to the conventional PTR-MS. Based on the laboratory evaluation by Riva  
62 et al. (2019a), the Vocus PTR-TOF is able to measure both monoterpenes and lots of monoterpene oxidation products  
63 containing up to 6 oxygen atoms.

64 Known for strong monoterpene emitters (Simon et al., 1994), the Landes forest in southwestern France is a suitable  
65 place to investigate atmospheric terpene chemistry. A previous study at this site reported a high nocturnal monoterpene loading  
66 and suggested that monoterpene oxidations play an important role in formation of new particles and the consequent growth of  
67 atmospheric particles (Kammer et al., 2018). To better assess the roles of BVOCs in aerosol formation, the Characterization  
68 of Emissions and Reactivity of Volatile Organic Compounds in the Landes Forest (CERVOLAND campaign) took place in  
69 July 2018. The recently developed Vocus PTR-TOF was deployed in the CERVOLAND campaign to characterize terpenes  
70 and their gas-phase oxidation products, which provides the first Vocus PTR-TOF measurement in a forested environment. In  
71 this work, we present a comprehensive summary of the identified gas-phase molecules and gain insights into terpene chemistry  
72 to demonstrate the Vocus PTR-TOF capabilities and the importance of its applications in atmospheric sciences.  
73 Characterizations of isoprene, monoterpenes, sesquiterpenes, and particularly the rarely detected diterpenes, are reported. By  
74 comparing the reaction rates of different formation pathways, we explore the formation mechanisms of terpene oxidation  
75 products, including both non-nitrate and organic nitrate compounds.

## 76 **2. Experimental methods**

### 77 **2.1 Measurement site**

78 The Vocus PTR-TOF measurements were performed from 8 to 20 July, 2018 in the Landes forest ( $44^{\circ}29'39.69''N$ ,  
79  $0^{\circ}57'21.75''W$ ), as part of the CERVOLAND field campaign. The sampling site is situated at the European Integrated Carbon  
80 Observation System (ICOS) station at Bilos in southwestern France along the Atlantic coast,  $\sim 40$  km southwest from the

81 nearest urban area of the Bordeaux metropole. Both population density and industrial emissions are low in this area. Due to  
82 the proximity of the Atlantic Ocean, the site has a strong maritime influence. The forest is largely composed of maritime pines  
83 (*Pinus pinaster* Aiton) and has an average height of ~10m. Monoterpenes are known to be strongly emitted in the forest (Simon  
84 et al., 1994), which provides a good place for BVOCs characterization. A more detailed description of the site has been  
85 provided in earlier studies (Moreaux et al., 2011; Kammer et al., 2018; Bsaibes et al., 2019).

## 86 **2.2 Instrumentation**

87 Compared to the conventional PTR instrument, the Vocus PTR-TOF used in this study is mainly differentiated in the following  
88 aspects:

- 89 1. a new chemical ionization source with a low-pressure reagent-ion source and focusing ion-molecule reactor (FIMR),
- 90 2. no dependence of the sensitivity on ambient sample humidity due to the high water mixing ratio (10-20 % v/v) in the  
91 FIMR,
- 92 3. employment of a TOF mass analyzer with a longer flight tube and faster sampling data acquisition card (mass  
93 resolving power up to 15 000 m/dm),
- 94 4. an enhanced inlet and source design that minimizes contact between analyte molecules and inlet/source walls,  
95 enabling detection of semi- and low-volatility compounds in a similar manner as chemical ionization mass  
96 spectrometer (CIMS) instruments (Liu et al. 2019).

97  
98 Details about the Vocus PTR-TOF are well described by Krechmer et al. (2018). Compared to the ionization in a conventional  
99 PTR-MS at 2.0-4.0 mbar, a nitrate CIMS at ambient pressure, and an iodide CIMS at around 100 mbar, the Vocus ionization  
100 source is generally operated at a low pressure (Krechmer et al., 2018). In this work, we operated the Vocus ionization source  
101 at a pressure of 1.5 mbar. During the campaign, the Vocus PTR-TOF measurements were performed at around 2 m above  
102 ground level (a.g.l), thus within the canopy. Sample air was drawn in through 1-m long PTFE tubing (10 mm o.d., 8 mm i.d.)  
103 with a flow rate of 4.5 L min<sup>-1</sup>, which helped to reduce inlet wall losses and sampling delay. Of the total sample flow, only  
104 150 sccm went into the Vocus, while the remainder was directed to the exhaust. The design of FIMR consists of a glass tube  
105 with a resistive coating on the inside surface and four quadrupole rods mounted radially on the outside. With an RF field, ions  
106 are collimated to the central axis, improving the detection efficiency of product ions. The mass resolving power of the 1.2 m  
107 long TOF mass analyzer was 12 000-13 000 m/dm during the whole campaign. Data were recorded with a time resolution of  
108 5 s. Background measurements using high purity nitrogen (UHP N<sub>2</sub>) were automatically performed every hour.

109 The temperature, relative humidity (RH), wind speed, and ambient pressure were continuously monitored at 3.4 m  
110 a.g.l. whereas the solar radiation was measured at 15.6 m a.g.l from a mast located at the site. The mixing ratios of nitrogen  
111 oxides (NO<sub>x</sub>) and ozone (O<sub>3</sub>) were measured at 4 m a.g.l with UV absorption and chemiluminescence analyzers, respectively.  
112 All data are reported in Coordinated Universal Time (UTC).

## 113 **2.3 Data analysis and quantification of multiple compounds**

114 Data analysis was performed using the software package “Tofware” (<https://www.tofwerk.com/software/tofware/>) that runs in  
115 the Igor Pro environment (WaveMetrics, OR, USA). Tofware enables the time-dependent mass calibration, baseline  
116 subtraction, and assignment of a molecular formula to the identified ions by high resolution analysis. Signals were averaged  
117 over 30 min before mass calibration. Due to the high resolving power of the LTOF mass analyzer, isobaric ions were more  
118 clearly separated. Examples of peak identification are given in Fig. S1.

119 The Vocus was calibrated twice a day during the campaign with a mixture (70 ppb each) of terpenes (*m/z* 137:  
120 alpha/beta pinene + limonene; *m/z* 135: *p*-cymene) that was diluted using UHP N<sub>2</sub>. Similar to conventional PTR instruments,  
121 the sensitivities of different VOCs in the Vocus PTR-TOF are linearly related to their proton-transfer reaction rate constants

122 ( $k$ ) when ion transmission efficiency and fragmentation ions are considered (Sekimoto et al., 2017; Krechmer et al., 2018).  
123 Krechmer et al. (2018) have shown that within the Vocus PTR-TOF, the transmission efficiencies of ions  $> m/z$  100 Th reach  
124 up to 99%. Therefore, the influence of fragmentation correction should be included in this study. According to terpene  
125 calibrations, the residual fraction was on average 66% and 55%, respectively, for protonated monoterpenes and  $p$ -cymene after  
126 their fragmentation within the instrument. Based on the corrected sensitivities for fragmentation and the  $k$  values of  
127 monoterpenes and  $p$ -cymene, an empirical relationship between the sensitivity and  $k$  was built from the scatterplots using linear  
128 regression: Sensitivity (cps ppb<sup>-1</sup>) =  $828.9 \times k$  (Fig. S2). Once  $k$  is available, the sensitivity of a compound can be predicted. It  
129 should be noted that the established relationship in this study is not applicable to other conditions or instruments. Some studies  
130 found that isoprene may fragment significantly to  $m/z$  41 (Keck et al., 2008; Schwarz et al., 2009). However, with the ambient  
131 data in this work, isoprene seems not to fragment much to  $C_3H_5^+$ , and they correlate poorly with each other (Fig. S3). Therefore,  
132 the fragmentation of isoprene is not considered for its quantification. Sesquiterpenes and some terpene oxidation products were  
133 found to fragment to varying degrees (Kim et al., 2009; Kari et al., 2018). Due to the lack of calibrations using other terpenes  
134 or terpene oxidation products, their fragmentation patterns within the Vocus PTR-TOF are not known in this work. Therefore,  
135 all the other terpenes and terpene oxidation products were quantified without consideration of fragment ions, which should be  
136 regarded as the lower limit of their ambient concentrations.

137 Rate constants for the proton-transfer reactions have only been measured for a subset of compounds. To quantify  
138 terpenes and their oxidation products, we used the method proposed by Sekimoto et al. (2017) to calculate the rate constants  
139 of different compounds with the polarizability and permanent dipole moment of the molecule. According to Sekimoto et al.  
140 (2017), the polarizability and dipole moment of a molecule can be obtained based on the molecular mass, elemental  
141 composition, and functionality of the compound. For a class of VOCs with the same number of electronegative atoms, their  
142 polarizabilities can be well described using their molecular mass (Sekimoto et al., 2017). For VOCs containing a specific  
143 functional group, it is found that their dipole moments are relatively constant based on results in the CRC Handbook (Lide,  
144 2005). Since no isomer information is provided by mass spectrometry alone, it is challenging to figure out the functionality of  
145 different compounds. Therefore, the polarizability and dipole moment of the compounds observed in this study were estimated  
146 only based on the molecular mass and elemental composition. In this work, based on the physical properties of various  
147 compounds in CRC Handbook (Lide, 2005) and the results in Sekimoto et al. (2017), we built the functions between  
148 polarizability ( $\alpha$ ) and molecular mass ( $M_R$ ) for different groups of VOCs and calculated the average dipole moment ( $\mu$ ) for  
149 each group. For example, the polarizabilities of hydrocarbons were approximated as  $\alpha = 0.142 M_R - 0.3$  and the dipole moment  
150 was approximated to be zero. For the non-nitrate oxygenated compounds with one oxygen,  $\alpha = 0.133 M_R - 1.2$ , and the dipole  
151 moment was averaged to be 1.6.

152 It should be noted that uncertainties are introduced to the calculated sensitivities in the following factors. Firstly, the  
153 small difference between the rate coefficients of monoterpenes and  $p$ -cymene may lead to large uncertainty in the established  
154 linear regression function between sensitivity and  $k$ . Calibrations with more VOC compounds should be performed in future  
155 works to cover a larger range of  $k$  values. Secondly, as mentioned above, the theoretically calculated sensitivities of  
156 sesquiterpenes, diterpenes, and terpene oxidation products, may be underestimated to varying extent without the consideration  
157 of their fragment ions. Further, some low-volatility compounds may experience wall losses inside the inlet tubing and the  
158 instrument and therefore have worse transmissions. The method in this work may overestimate the sensitivities of these low-  
159 volatility compounds. In addition to proton transfer reactions, some VOCs can be ionized through ligand switching reactions  
160 with water cluster ( $(H_2O)_nH_3O^+$ ) (Tani et al., 2004), thus increasing their sensitivity. However, with the calibration standards  
161 used in this study, it is hard to estimate the effect of ligand switching ionization. Lastly, uncertainties come from the estimation  
162 of polarizability and dipole moment of a molecule. With the method used in this study, the sensitivity is calculated to be within  
163 50% error when only the elemental composition of a compound is known (Sekimoto et al., 2017).

### 164 3. Results and discussion

#### 165 3.1 Meteorology and trace gases

166 Figure 1 displays the time variations of meteorological conditions and trace gases during the observation period. The weather  
167 was mostly sunny, with solar radiation varying from 400 to 800 W/m<sup>2</sup> during daytime, indicating strong photochemical activity.  
168 The ambient temperature and RH varied regularly every day. On average, the temperature was 22.8 ± 5.9 °C (mean ± SE),  
169 ranging from 12.1 to 35.0 °C, which is favorable for BVOCs emissions in the forest. The average RH was 70.5 ± 19.0 % during  
170 the campaign. Generally, the air masses were quite stable within the canopy. The wind speed never exceeded 1 m/s, indicating  
171 the major influence of local sources on atmospheric processes in this study.

172 The O<sub>3</sub> levels fluctuated dramatically between day and night during the campaign. The average O<sub>3</sub> diurnal cycle  
173 showed that O<sub>3</sub> concentration peaked up to ~50 ppb in the daytime. However, during most of the nights, O<sub>3</sub> concentration  
174 dropped below 2 ppb. Considering the high nighttime concentration of terpenes observed by the previous study at this site in  
175 the same season (Kammer et al., 2018), the low O<sub>3</sub> level at night suggests the large consumption of O<sub>3</sub> by terpenes. Such  
176 reactions of terpenes with O<sub>3</sub> can produce low volatility organic compounds, thus contributing to SOA formation (Presto et al.,  
177 2005; Jokinen et al., 2014). In addition, plant surface uptake is likely another important ozone sink in the canopy (Goldstein  
178 et al., 2004).

179 The NO concentration was generally low during the campaign, below detection limit (i.e., <0.5 ppb) most of the time.  
180 However, clear NO plumes was sometimes observed in the early morning, as shown in Fig.1e. The NO concentration peak at  
181 4 am is probably the combination of local emission sources and low boundary layer. With the increasing sunlight afterwards,  
182 the NO concentration started to decrease. A similar diel pattern of NO<sub>2</sub> was observed by the previous study at this site (Kammer  
183 et al., 2018). The lower NO<sub>2</sub> concentration during daytime is likely explained by dilution with increasing boundary layer height  
184 and NO<sub>2</sub> photolysis.

#### 185 3.2 Vocus PTR-TOF capabilities in the forest

186 While Krechmer et al. (2018) and Riva et al. (2019a) have described the novel setup and performance of the Vocus PTR-TOF  
187 and its application during a lab study, the instrument capability has not been fully explored in an ambient environment. Based  
188 on the CERVOLAND deployment, we provide here, the first overview of gas-phase molecules measured by the Vocus PTR-  
189 TOF in the forest. For a better visualization of the complex data set from real atmosphere, mass defect plots (averaged over  
190 the whole campaign) are shown in Fig. 2 with the difference between the exact mass and the nominal mass of a compound  
191 plotted against its exact mass. With the addition of hydrogen atoms, the mass defect increases, while the addition of oxygen  
192 atoms decreases the mass defect. Therefore, changes in the mass defect plot help to provide information on chemical  
193 transformation such as oxidation.

194 The mass defect plot in Fig. 2a is colored according to the retrieved elemental composition, with the black circle  
195 indicating unidentified molecules. The size of the markers is proportional to the logarithm of the peak area of the molecule.  
196 During the campaign, the Vocus PTR-TOF detected large amounts of (O)VOCs, with elemental composition categories of CH,  
197 CHO, CHN, CHS, CHON, CHOS, and others. For hydrocarbons, multiple series with different carbon numbers were measured,  
198 especially those compounds containing 5 (“C<sub>5</sub>”) to 10 carbon atoms (“C<sub>10</sub>”), 15 carbon atoms (“C<sub>15</sub>”), and 20 carbon atoms  
199 (“C<sub>20</sub>”). Some of the C<sub>5</sub> – C<sub>9</sub> ions can be fragments of terpenes and their oxidation products (Tani et al., 2003, 2013; Kim et  
200 al., 2009; Kari et al., 2018). For ions <35 Th, the detection efficiency is much reduced due to a high-pass band filter of the  
201 BSQ (Krechmer et al., 2018). Compared to the conventional PTR instruments, the observation of larger hydrocarbon molecules  
202 by the Vocus PTR-TOF is mainly caused by the much lower wall losses and increased detection efficiency. Hydrocarbon  
203 signals were largely contributed by monoterpene (C<sub>10</sub>H<sub>16</sub>H<sup>+</sup>) and its major fragment (C<sub>6</sub>H<sub>8</sub>H<sup>+</sup>), indicating the monoterpene-  
204 dominated environment in the Landes forest (Kammer et al., 2018). According to previous studies, monoterpene emissions in

205 the Landes forest are dominated by  $\alpha$ -pinene and  $\beta$ -pinene (Simon et al., 1994; Kammer et al., 2018). The identified compound  
206 with the elemental composition of  $C_4H_9^+$  ranked the third largest peak in hydrocarbons. Detailed discussion about  $C_4H_9^+$  ions  
207 can be found in the supplement.

208 In addition to the emitted precursors, the Vocus PTR-TOF detected various VOCs reaction products and  
209 intermediates. Similar to the PTR3 measurements in the CLOUD chamber (Breitenlechner et al., 2017), many oxygenated  
210 compounds from terpene reactions with varying degrees of oxidation were observed in this study. However, as a potential  
211 limitation of the instrument, no dimers in the atmosphere were identified by the Vocus PTR-TOF, consistent with the results  
212 from a previous laboratory deployment (Riva et al., 2019a).

213 Figure 2b compares the daytime and nighttime variations of different molecules, with the marker sized by the signal  
214 difference between day and night. The daytime periods cover from 4:30 am to 7:30 pm, and the nighttime periods are from  
215 7:30 pm to 4:30 am of the next day (both are UTC time; Local time = UTC time + 2). The data points are colored in orange  
216 when the nighttime signal of the compound is larger than its daytime signal, and in green when the daytime signal is higher.  
217 Patterns in the figure clearly show the difference in the diurnal variations of gas molecules with different oxidation degrees.  
218 For example, most hydrocarbons are characterized with higher concentrations at night, which is largely caused by the stable  
219 nocturnal boundary layer. The more oxidized compounds with more oxygen numbers are generally more abundant during the  
220 day due to enhanced photochemistry, whereas the concentrations of the less oxidized compounds are mostly higher at night.  
221 Details on the diurnal profiles of different oxidation products and their formation mechanisms are provided in Sect. 3.4.

### 222 3.3 Terpene characteristics

223 The characterizations of isoprene, monoterpenes, sesquiterpenes, and the rarely reported diterpenes, are investigated in this  
224 study (Fig. 3, Fig. 4). On the global scale, isoprene is the most emitted BVOC species. It has been well established that  
225 photooxidation of isoprene in the atmosphere contributes to SOA formation through the multiphase reactions of isoprene-  
226 derived oxidation products (Claeys et al., 2004; Henze and Seinfeld, 2006; Surratt et al., 2010). However, recent advances on  
227 isoprene chemistry found that isoprene can impact both particle number and mass of monoterpene-derived SOA by scavenging  
228 hydroxyl and peroxy radicals (Kiendler-Scharr et al., 2009; Kanawade et al., 2011; McFiggans et al., 2019). During the  
229 CERVOLAND campaign, the average mixing ratio of isoprene was 0.6 ppb, consistent with the mean value of 0.4 ppb reported  
230 for the LANDEX campaign during summer 2017 at the same site (Mermet et al., 2019). These values are much lower than that  
231 in the southeastern United States (Xiong et al., 2015) and Amazon rainforest (Wei et al., 2018) but higher than observations  
232 in the boreal forest at the SMEAR II station (Hellén et al., 2018). Isoprene emissions are strongly light-dependent (Monson et  
233 al., 1989; Kaser et al., 2013). Therefore, a pronounced diurnal pattern of isoprene was observed with maximum mixing ratios  
234 occurring during daytime and minima at night. It has been shown that the attribution of  $C_5H_9^+$  ions to isoprene with PTR  
235 instruments can be influenced by the fragmentation of many other compounds, i.e., cycloalkane and 2-methyl-3-buten-2-ol  
236 (MBO) (Karl et al., 2012; Gueneron et al., 2015). For example, using an  $E/N$  ratio of 106 Td in the PTR-MS with a quadrupole  
237 mass analyzer, 71% of the parent MBO fragmented to  $C_5H_9^+$  ions (Warneke et al., 2003). However, in this study, the  $C_5H_9^+$   
238 signal was around 10 times as high as the  $C_5H_{11}O^+$  signal and both ions correlated poorly with each other (Fig. S4;  $r^2 = 0.33$ ).  
239 This information demonstrate that the fragmentation of MBO does not likely have a significant influence on the attribution of  
240  $C_5H_9^+$  ions to isoprene in this work.

241 As expected, monoterpenes showed the highest mixing ratios among all the terpenes, with an average value of 6.0  
242 ppb. On July 9, a heavy monoterpene episode occurred at night, with the monoterpene mixing ratio reaching as high as 41.2  
243 ppb. Comparatively, the average monoterpene level observed in this work is similar to the measurements performed in 2015  
244 and 2017 at the same site (Kammer et al., 2018; Mermet et al., 2019) and more than ten times higher than that observed in the  
245 boreal forest at SMEAR II in summer (Hakola et al., 2012; Hellén et al., 2018). The high concentration of monoterpenes  
246 indicates the potential significance of monoterpene-related aerosol chemistry in the Landes forest. Different from the light-

247 dependence of isoprene emissions, monoterpene emissions are found to be mainly controlled by temperature (Hakola et al.,  
248 2006; Kaser et al., 2013). At night, monoterpenes can be continuously emitted and accumulated within the boundary layer.  
249 Therefore, monoterpenes showed the opposite diel pattern to isoprene and peaked during nighttime. During daytime, the  
250 concentration of monoterpenes dropped to around 0.9 ppb, due to the increased atmospheric mixing after sunrise and the rapid  
251 photochemical consumptions.

252 A study in Hyytiälä concluded that sesquiterpenes, due to their higher reactivity, could play a more important role in  
253 O<sub>3</sub> chemistry than monoterpenes, even though the concentration of sesquiterpenes was much lower (Hellén et al., 2018).  
254 However, the short lifetimes of sesquiterpenes also mean that their concentrations will be highly dependent on the sampling  
255 location at a given site. Some studies also proposed that sesquiterpene oxidation products are linked to atmospheric new particle  
256 formation (Bonn and Moortgat, 2003; Boy et al., 2007). Despite the potential importance of sesquiterpenes in aerosol chemistry,  
257 the available data on ambient sesquiterpene quantification remains still quite limited. In this work, the mixing ratios of  
258 sesquiterpenes were found to vary from 8.9 ppt to 408.9 ppt in the Landes forest, with an average of 64.5 ppt during the  
259 observations. This sesquiterpene level is comparable to that reported by Mermert et al. (2019) in summer 2017 at the same site  
260 and observations by Jardine et al. (2011) in Amazonia but higher than previous measurements at SMEAR II station (Hellén et  
261 al., 2018). Kim et al. (2009) show that different sesquiterpenes fragment on monoterpene parent and fragment ions to varying  
262 degrees inside the PTR instruments. Without the consideration of sesquiterpene fragmentation, the quantification of  
263 sesquiterpenes in this work may be underestimated. As shown in Fig. 4, sesquiterpenes displayed a similar diurnal pattern with  
264 monoterpenes, consistent with observations in other areas (Jardine et al., 2011; Hellén et al., 2018).

265 While diterpenes are present in all plants in the form of phytol, they have been thought for a long time not to be  
266 released by vegetation due to their low volatility (Keeling and Bohmann, 2006). In 2004, von Schwartzberg et al. (2004)  
267 reported for the first time the release of plant-derived diterpenes into the air. A recent study found that the emission rate of  
268 diterpenes by Mediterranean vegetation was in the same order of magnitude as monoterpenes and sesquiterpenes (Yáñez-  
269 Serrano et al., 2018). For the first time, this study reports the ambient concentration of diterpenes in a forest. According to the  
270 Vocus PTR-TOF measurements, the average mixing ratio of diterpenes was around 2 ppt in the Landes forest. Considering the  
271 low volatility of diterpenes and their potential wall losses inside the inlet tubing and the instrument, the diterpene concentration  
272 might be higher. Similar to monoterpenes and sesquiterpenes, diterpenes presented peak concentrations at night and lower  
273 levels during the day. Although the amounts of diterpenes in the atmosphere are hundreds to thousands times lower than those  
274 of monoterpenes and sesquiterpenes, diterpenes potentially play a role in atmospheric chemistry due to their unsaturated  
275 structure and high molecular weight (Matsunaga et al., 2012). Up to now, there is no report on the possible atmospheric  
276 implications of diterpenes, which should deserve more attention in the future.

277 Considering the similar atmospheric behaviors of monoterpenes, sesquiterpenes, and diterpenes in this study, it is  
278 questioned if the observed sesquiterpenes and diterpenes are real signals in the atmosphere or generated by monoterpenes in  
279 the instrument. Bernhammer et al. (2018) have shown that secondary association reactions of protonated isoprene with isoprene  
280 can form monoterpenes within the PTR reaction chamber. Figure 5 illustrates the scatter plots among monoterpenes,  
281 sesquiterpenes, and diterpenes, colored by time of the day. At night, both sesquiterpenes and diterpenes correlated well with  
282 monoterpenes. However, their correlation with monoterpenes got weaker during daytime as the data points became more  
283 scattered. This suggests that the observations of sesquiterpenes and diterpenes are real emissions in the atmosphere.  
284 Comparatively, sesquiterpenes and diterpenes showed a strong correlation with each other through the whole day ( $r^2 = 0.85$ ).

### 285 **3.4 Insights into terpene chemistry**

#### 286 **3.4.1 Comparison with chamber results**

287 Due to the diverse precursors and changing environmental conditions in the ambient air, it is challenging to retrieve all the  
288 atmospheric chemical processes occurring within the Landes forest. To start with, we compare the ambient data with those

289 from  $\alpha$ -pinene ozonolysis in the presence of  $\text{NO}_x$  conducted in the COALA chamber at the University of Helsinki. A detailed  
290 description of the laboratory experiment is provided elsewhere (Riva et al., 2019a, 2019b). According to literature,  
291 monoterpenes undergo some degree of fragmentation within the PTR instrument, producing dominant ions of  $\text{C}_6\text{H}_9^+$ ,  $\text{C}_5\text{H}_7^+$ ,  
292  $\text{C}_7\text{H}_{11}^+$ , et al (Tani et al., 2003, 2013; Kari et al., 2018). As illustrated in Fig. 6,  $\text{C}_6\text{H}_9^+$  is the largest fragment produced by  
293 monoterpenes within the Vocus PTR-TOF. However, a clear difference of monoterpene fragmentation pattern is observed in  
294 the mass spectra of ambient observations and chamber experiments. While the signal of  $\text{C}_6\text{H}_9^+$  is lower than that of  $\text{C}_{10}\text{H}_{17}^+$   
295 during the field deployment,  $\text{C}_6\text{H}_9^+$  peak is higher than  $\text{C}_{10}\text{H}_{17}^+$  peak in the chamber study. Based on the monoterpene  
296 calibration data, the  $\text{C}_6\text{H}_9^+$  signal is around 40% and 138% of the protonated monoterpene signal in ambient deployment and  
297 chamber experiment, respectively. The larger presence of the  $\text{C}_6\text{H}_9^+$  peak in the chamber study can be likely explained by the  
298 much higher concentrations of oxygenated terpenoids during the chamber experiments. Indeed, previous studies have shown  
299 that oxygenated terpenoids, including linalool and pinonaldehyde, fragment inside the PTR instrument and produce a dominant  
300 ion at  $m/z$  81 (Maleknia et al., 2007; Tani, 2013). Different settings of the instrument can also contribute to different  
301 fragmentation patterns of monoterpenes (Tani et al., 2003, 2013; Kari et al., 2018). In our ambient and chamber studies, the  
302  $E/N$  values of the Vocus PTR-TOF are quite similar, 118 Td and 120 Td, respectively. In addition, the fragmentation patterns  
303 vary among individual monoterpene species due to their different physicochemical properties (Tani et al., 2013; Kari et al.,  
304 2018). Considering that  $\alpha$ -pinene is the only monoterpene species injected in the chamber experiment, the combination of  
305 various monoterpenes in the atmosphere likely introduces additional differences in the fragmentation pattern.

306 Gas-phase ozonolysis of alkenes generates OH radicals in high yields (Rickard et al., 1999). Without an OH scavenger,  
307 both  $\text{O}_3$ - and OH-initiated oxidations happened during  $\alpha$ -pinene ozonolysis in the chamber. Using the Vocus PTR-TOF,  
308 various oxidation products were identified in the chamber study, with the dominant species being  $\text{C}_7\text{H}_{10,12}\text{O}_{3-6}$ ,  $\text{C}_8\text{H}_{14}\text{O}_{3-6}$ ,  
309  $\text{C}_9\text{H}_{14}\text{O}_{1-5}$ , and  $\text{C}_{10}\text{H}_{14,16}\text{O}_{2-6}$ . In comparison, more oxygenated compounds which were directly emitted or from monoterpene  
310 reactions were observed in ambient air due to complex environmental conditions, with the oxygen number ranging from 1 to  
311 7. Therefore, the Vocus PTR-TOF measurements provide the opportunity to characterize both the emitted precursors and the  
312 resulting oxidation products. During the chamber experiments,  $\text{NO}_2$  was injected and photolyzed using 400nm LED lights to  
313 generate NO. In the presence of  $\text{NO}_x$ , organic nitrates were formed from the reactions between NO and monoterpene-derived  
314 peroxy radicals ( $\text{RO}_2$ ). The major organic nitrates observed were  $\text{C}_9\text{H}_{13,15}\text{NO}_{6-8}$  and  $\text{C}_{10}\text{H}_{13,15}\text{NO}_{3-8}$ . Compared to the chamber  
315 study, more organic nitrates of  $\text{C}_8$ ,  $\text{C}_9$ , and  $\text{C}_{10}$  from monoterpene reactions were identified in CERVOLAND data. It is worth  
316 pointing out that the combination of different monoterpene species in the ambient environment may result in various types of  
317 organic nitrates through different formation pathways.

### 318 3.4.2 Non-nitrate terpene oxidation products

319 Based on the ambient observations, the non-nitrate oxidation products from isoprene, monoterpenes, and sesquiterpenes, are  
320 investigated in this study. Isoprene gas-phase products are mainly represented by  $\text{C}_4$  and  $\text{C}_5$  compounds (Wennberg et al.,  
321 2018). In this work, we consider  $\text{C}_4\text{H}_{6,8}\text{O}_n$  and  $\text{C}_5\text{H}_{8,10,12}\text{O}_n$  ( $n=1\sim 6$ ) as the dominant non-nitrate products from isoprene  
322 oxidations. The diurnal variations of  $\text{C}_5\text{H}_8\text{O}_n$  are displayed in Fig. 7 and the others in Fig. S5-7. Generally, all these oxidation  
323 products displayed an evening peak at around 8 pm, which may come from the  $\text{O}_3$ - or OH-initiated isoprene oxidations.  
324 Reaction with OH represents the largest loss pathway for isoprene in the atmosphere and produces a population of isoprene  
325 peroxy radicals (Wennberg et al., 2018). In the presence of NO, the major products are methyl vinyl ketone (MVK,  $\text{C}_4\text{H}_6\text{O}$ )  
326 and methacrolein (MACR,  $\text{C}_4\text{H}_6\text{O}$ ). Globally, reactions with  $\text{O}_3$  contribute a small fraction of approximately 10% to isoprene  
327 removal in the atmosphere (Wennberg et al., 2018). When isoprene reacts with  $\text{O}_3$ , one carbon is always split off from the  
328 molecule (Criegee, 1975). Considering the peak concentration of isoprene at 8 pm and the relatively high  $\text{O}_3$  concentration at  
329 the moment (Figs. 1 and 4), isoprene ozonolysis is also likely contributing to the formation of  $\text{C}_4$  oxidation products. Because  
330 OH radicals can be efficiently produced from alkene ozonolysis (Pfeiffer et al., 2001), the OH-initiated oxidation of isoprene



331 can also be an important formation pathway of these oxidation products in the evening. For example, as a predominant product  
332 from the reactions of isoprene with OH, C<sub>5</sub>H<sub>10</sub>O<sub>3</sub> (corresponding to isoprene hydroxy hydroperoxide and/or isoprene  
333 epoxydiols) presented a clear single peak in the evening. To determine the relative importance of O<sub>3</sub>- and OH-initiated  
334 oxidations in isoprene chemistry at night, the reaction rates (R) of isoprene with O<sub>3</sub> and OH radical were compared by Eq. (1)  
335 and Eq. (2):

$$336 R_{\text{ISO+OH}} = k_{\text{ISO+OH}}[\text{ISO}][\text{OH}] \quad (1)$$

$$337 R_{\text{ISO+O}_3} = k_{\text{ISO+O}_3}[\text{ISO}][\text{O}_3] \quad (2)$$

338 where *k* is the reaction rate coefficient of isoprene with OH or O<sub>3</sub>, and [ISO], [OH] or [O<sub>3</sub>] is the concentration of isoprene,  
339 OH radical or O<sub>3</sub>.

340 Taking the evening peak of isoprene oxidation products at 8 pm as an example, we compared the roles of O<sub>3</sub> and OH radicals  
341 in their formation. Laboratory studies have shown that the reaction rate coefficient of isoprene with OH radical is generally  
342 10<sup>7</sup> times larger than that of isoprene with O<sub>3</sub> (Dreyfus et al., 2002; Kari et al., 2004). Based on the competition between OH  
343 production and removal processes at night (Dusanter et al., 2008), the steady state OH concentration was estimated to be 0.012  
344 ppt. Details can be found in the supplement. With an O<sub>3</sub> concentration of ~20 ppb at 8 pm, the reaction rate of isoprene with  
345 OH radical was around 6 times as high as that of isoprene with O<sub>3</sub>. For the more oxidized compounds from isoprene oxidations,  
346 their concentrations had a broad daytime presence from 10 am to 8 pm due to strong photooxidation processes. Similar diurnal  
347 variations of C<sub>4</sub>H<sub>6,8</sub>O<sub>5,6</sub> and C<sub>5</sub>H<sub>8,10,12</sub>O<sub>5,6</sub> measured by nitrate CIMS have been observed in an isoprene-dominated environment  
348 at Centreville, Alabama (Massoli et al., 2018).

349 The diurnal patterns of C<sub>8</sub>H<sub>12,14</sub>O<sub>n</sub>, C<sub>9</sub>H<sub>14</sub>O<sub>n</sub>, and C<sub>10</sub>H<sub>14,16,18</sub>O<sub>n</sub> (n=1~6) were illustrated to characterize monoterpene  
350 oxidations in the Landes forest (Fig. 8; Fig. S8-12). For the less oxidized compounds with oxygen numbers from 1 to 4, most  
351 of them were observed with clear morning and evening peaks, which can be produced from O<sub>3</sub>- and OH-initiated monoterpene  
352 oxidations. For the morning peak at around 7 am, the relative roles of O<sub>3</sub>- and OH-initiated monoterpene oxidation were  
353 evaluated using the similar method as in Eq. (1) and Eq. (2). The reaction rate coefficient of monoterpene + OH is  
354 approximately 10<sup>6</sup> times higher than that of monoterpene + O<sub>3</sub> (Atkinson et al., 1990; Khamaganov and Hites, 2001; Gill and  
355 Hites, 2002; Hakola et al., 2012). In the morning, typical tropospheric OH concentrations have been observed to be around 1  
356 × 10<sup>5</sup> – 1 × 10<sup>6</sup> molecule cm<sup>-3</sup> (0.004 – 0.04 ppt) (Shirinzadeh et al., 1987; Ren et al., 2003; Khan et al., 2008; Petäjä et al.,  
357 2009; Stone et al., 2012). For an OH concentration of 1 × 10<sup>5</sup> molecule cm<sup>-3</sup> (0.004 ppt), with the average O<sub>3</sub> concentration of  
358 15 ppb at 7 am, the reaction rate of monoterpene + OH was about 0.25 times as high as that of monoterpene + O<sub>3</sub>. If the OH  
359 concentration was up to 1 × 10<sup>6</sup> molecule cm<sup>-3</sup> (0.04 ppt) at 7 am, the reaction rate of monoterpene with OH radical was 2.5  
360 times higher than that of monoterpene with O<sub>3</sub> according to the calculations. In other words, both oxidants are likely to be of  
361 importance at this time. For the evening peak of the less oxidized monoterpene oxidation products at 8 pm, the relative  
362 importance of O<sub>3</sub> and OH radical in monoterpene chemistry changed due to the lower OH concentration. With the average O<sub>3</sub>  
363 concentration of ~20 ppb and OH concentration of 0.012 ppt at 8 pm, the reaction rates of monoterpenes with O<sub>3</sub> and OH  
364 radical were at the similar level. Compared to other compounds, the evening peak of C<sub>9</sub>H<sub>14</sub>O, C<sub>10</sub>H<sub>16</sub>O, C<sub>10</sub>H<sub>18</sub>O, and C<sub>10</sub>H<sub>18</sub>O<sub>2</sub>  
365 extended over midnight. C<sub>9</sub>H<sub>14</sub>O has been found to be one of the main products formed in the ozonolysis reactions of  
366 monoterpenes (Atkinson and Arey, 2003). O<sub>3</sub>-initiated oxidation with extremely high monoterpene levels might be responsible  
367 for the high concentration of C<sub>9</sub>H<sub>14</sub>O at night. Camphor (C<sub>10</sub>H<sub>16</sub>O), linalool (C<sub>10</sub>H<sub>18</sub>O), and linalool oxide (C<sub>10</sub>H<sub>18</sub>O<sub>2</sub>) can be  
368 emitted by leaves and flowers (Corchnoy et al., 1992; Lavy et al., 2002). Therefore, direct emissions from vegetation in the  
369 Landes forest may contribute to the high mixing ratios of these compounds during night. With strong photochemical oxidations  
370 during the day, the diurnal cycles of the more oxidized compounds were characterized with a broad daytime distribution  
371 peaking between 2:00 pm and 4:00 pm UTC.

372 To date the oxidation processes of sesquiterpenes have been rarely investigated despite its potential significance in  
373 new particle formation and SOA formation (Bonn and Moortgat, 2003; Winterhalter et al., 2009). In this study, various

374 sesquiterpene oxidation products were observed, mainly including  $C_{14}H_{22}O_n$ ,  $C_{15}H_{22}O_n$ , and  $C_{15}H_{24}O_n$  ( $n=1\sim6$ ), providing the  
375 possibility to explore the oxidations of sesquiterpenes in the atmosphere. As shown in Fig. 9 and Fig. S13-14, with the increase  
376 of oxygen numbers, sesquiterpene oxidation products displayed similar variations in their diurnal profiles with monoterpene  
377 oxidation products. The less oxidized products with 1 to 3 oxygen peaked both in the morning and in the evening, and the  
378 more oxidized compounds had a broad presence throughout the day. These results indicate the similar oxidation processes of  
379 sesquiterpenes with monoterpenes in the Landes forest.

### 380 3.4.3 Terpene-derived organic nitrates

381 Organic nitrates have been shown to represent a large fraction of submicron aerosol nitrate at both urban and rural sites in  
382 Europe (Kiendler-Scharr et al., 2016). During daytime, the reaction of peroxy radicals with NO can lead to the formation of  
383 organic nitrates. At night,  $NO_3$  radicals from the oxidation of  $NO_2$  by  $O_3$ , can also react with unsaturated compounds mostly  
384 coming from BVOCs to generate organic nitrates (Ayres et al., 2015). In this study, the less oxidized organic nitrates from  
385 monoterpene oxidations presented a distinct morning peak at 7 am (Fig. 11; Fig. S17-18), which can come from  $O_3$ - and OH-  
386 initiated monoterpene oxidations in the presence of  $NO_x$ . In addition, both isoprene- and monoterpene-derived organic nitrates  
387 showed evening peaks at around 8 pm (Fig. 10, Fig. S15-16). Using monoterpenes as an example, the relative roles of  $O_3$ , OH  
388 radical, and  $NO_3$  radical in the nighttime formation of monoterpene-derived organic nitrates were evaluated by calculating the  
389 corresponding reaction rate (R):

$$390 R_{MT+O_3} = k_{MT+O_3}[MT][O_3] \quad (3)$$

$$391 R_{MT+OH} = k_{MT+OH}[MT][OH] \quad (4)$$

$$392 R_{MT+NO_3} = k_{MT+NO_3}[MT][NO_3] \quad (5)$$

393 where  $k$  is the reaction rate coefficient of monoterpenes with  $O_3$ , OH radical or  $NO_3$  radical, and [MT],  $[O_3]$ , [OH] or  $[NO_3]$  is  
394 the concentration of monoterpenes,  $O_3$ , OH radical or  $NO_3$  radical.

395 Taking the peak concentration of monoterpene-derived organic nitrates at 8 pm as an example, the concentration of  $NO_3$  radical  
396 was calculated by assuming a steady state between its production from  $O_3$  and  $NO_2$  and its removal by oxidation reactions and  
397 losses. The details have been described by Allan et al. (2000) and Peräkylä et al. (2014). With the high  $O_3$  scavenging by  
398 monoterpenes in the evening, the estimated concentration of  $NO_3$  radical was 0.017 ppt. Using  $k_{MT+O_3} = 6.9 \times 10^{-17} \text{ cm}^3$   
399  $\text{molecule}^{-1} \text{ s}^{-1}$  and  $k_{MT+NO_3} = 7.5 \times 10^{-12} \text{ cm}^3 \text{ molecule}^{-1} \text{ s}^{-1}$  taken from Peräkylä et al. (2014), the reaction rate of monoterpenes  
400 with  $O_3$  was ~10 times higher than that of monoterpenes with  $NO_3$  radicals. However, while ozonolysis was likely to dominate  
401 the overall oxidation of monoterpenes, the organic nitrate formation from  $O_3$ -initiated oxidation may still be much lower than  
402 those from  $NO_3$ -initiated oxidations, depending on what fraction of  $RO_2$  radicals were reacting with  $NO_x$ . The relative  
403 importance of  $O_3$  and OH radical in monoterpene chemistry at this time was the same as discussed in Sect. 3.4.2.

## 404 4. Conclusions

405 This work presented the deployment of the new state-of-the-art Vocus PTR-TOF in the French Landes forest during the  
406 CERVOLAND campaign. The Vocus PTR-TOF capabilities are evaluated for the first time in the actual ambient environment  
407 by the identification of the observed gas-phase molecules. With the improved detection efficiency and measurement precision  
408 compared to the conventional PTR instruments, multiple hydrocarbons with carbon numbers varying from 3 to 20 were  
409 observed as well as various VOCs oxidation products. Hydrocarbon signals were dominated by monoterpenes and their major  
410 fragment ions (e.g.,  $C_6H_8H^+$ ) within the instrument, consistent with high monoterpene emissions in the Landes forest. In general,  
411 most hydrocarbon molecules and the less oxidized compounds were characterized with high signals at night, whereas the more  
412 oxidized compounds exhibited elevated intensity during the day.

413 To demonstrate the importance of Vocus PTR-TOF application in atmospheric science study, the characteristics of  
414 terpenes and their oxidation products were investigated. In addition to the observation of isoprene, monoterpenes, and  
415 sesquiterpenes, this study presented the ambient characteristics of the rarely recorded diterpenes, which are traditionally  
416 considered as non-volatile species in the atmosphere. On average, the concentration of diterpenes was 1.7 ppt in the Landes  
417 forest, which was hundred to thousand times lower than that of monoterpenes (6.0 ppb) and sesquiterpenes (64.5 ppt). However,  
418 considering their low vapor pressure and high reactivity, diterpenes may potentially play an important part in atmospheric  
419 chemistry. The diurnal variations of diterpenes showed the maximum peak at night and low levels during the day, similar to  
420 those of monoterpenes and sesquiterpenes.

421 With strong photochemical oxidations of terpenes during the day, the more oxidized terpene reaction products were  
422 observed with a broad daytime peak, whereas the less oxidized terpene reaction products showed peak concentrations in the  
423 early morning or/and in the evening. By calculating the reaction rates of terpenes with the main oxidants, OH radical, O<sub>3</sub>, and  
424 NO<sub>3</sub> radical, the contributions of different formation pathways to terpene oxidations were evaluated. The morning and evening  
425 peaks of non-nitrate terpene reaction products were contributed by both O<sub>3</sub>- and OH-induced terpene oxidations. For the  
426 formation of terpene-derived organic nitrates, the relative importance of O<sub>3</sub>-, OH-, and NO<sub>3</sub>- driven oxidation pathways were  
427 more difficult to evaluate. Overall, we have shown that the Vocus PTR-TOF is able to detect a very broad coverage of  
428 compounds, from VOCs precursors to various oxidation products. Therefore, the application of the Vocus PTR-TOF in  
429 atmospheric sciences will be fundamental in understanding the chemical evolution of VOCs in the atmosphere and their roles  
430 in air quality and climate issues.

#### 431 **Author contributions**

432 ME and MR conceived the study. MR, LH, PF, EV, and EP conducted the field measurements. HL carried out the data analysis.  
433 MR, PR, KD, JK, DW, MK, ME, and FB participated the data analysis. HL wrote the paper with inputs from all coauthors.

#### 434 **Competing interests**

435 The authors declare that they have no conflict of interest.

#### 436 **Acknowledgements**

437 This work was supported by the European Research Council under grants 742206 ATM-GP, 638703 COALA and 850614  
438 CHAPAs, and the Academy of Finland (project numbers 317380 and 320094). The authors would like to thank the  
439 PRIMEQUAL programme for financial support (ADEME, convention #1662C0024). This study has also been carried out with  
440 financial support from the French National Research Agency (ANR) in the frame of the Investments for the future Programme,  
441 within the Cluster of Excellence COTE (ANR-10-LABX-45) of the University of Bordeaux. Special thanks to Dr Elena  
442 Ormeño-Lafuente (IMBE) for the loan of the BVOC calibration gas cylinders and Dr Christophe Chipeaux and Dr Denis  
443 Loustau (ISPA-INRA) for their precious help in providing meteorological data and access to ICOS station facility.

#### 444 **References**

- 445 Atkinson, R., Hasegawa, D., and Aschmann, S. M.: Rate constants for the gas-phase reactions of O<sub>3</sub> with a series of  
446 monoterpenes and related compounds at 296 ± 2 K, *International Journal of Chemical Kinetics*, 22, 871-887,  
447 10.1002/kin.550220807, 1990.
- 448 Atkinson, R., and Arey, J.: Atmospheric Degradation of Volatile Organic Compounds, *Chem Rev*, 103, 4605-4638,  
449 10.1021/cr0206420, 2003.

450 Ayres, B. R., Allen, H. M., Draper, D. C., Brown, S. S., Wild, R. J., Jimenez, J. L., Day, D. A., Campuzano-Jost, P., Hu, W.,  
451 de Gouw, J., Koss, A., Cohen, R. C., Duffey, K. C., Romer, P., Baumann, K., Edgerton, E., Takahama, S., Thornton, J. A.,  
452 Lee, B. H., Lopez-Hilfiker, F. D., Mohr, C., Wennberg, P. O., Nguyen, T. B., Teng, A., Goldstein, A. H., Olson, K., and Fry,  
453 J. L.: Organic nitrate aerosol formation via  $\text{NO}_3$  + biogenic volatile organic compounds in the southeastern  
454 United States, *Atmos. Chem. Phys.*, 15, 13377-13392, 10.5194/acp-15-13377-2015, 2015.

455 Baltensperger, U., Kalberer, M., Dommen, J., Paulsen, D., Alfarra, M. R., Coe, H., Fisseha, R., Gascho, A., Gysel, M., Nyeki,  
456 S., Sax, M., Steinbacher, M., Prevot, A. S. H., Sjögren, S., Weingartner, E., and Zenobi, R.: Secondary organic aerosols from  
457 anthropogenic and biogenic precursors, *Faraday Discussions*, 130, 265-278, 10.1039/B417367H, 2005.

458 Bernhammer, A. K., Fischer, L., Mentler, B., Heinritzi, M., Simon, M., and Hansel, A.: Production of highly oxygenated  
459 organic molecules (HOMs) from trace contaminants during isoprene oxidation, *Atmos. Meas. Tech.*, 11, 4763-4773,  
460 10.5194/amt-11-4763-2018, 2018.

461 Bertram, T. H., Kimmel, J. R., Crisp, T. A., Ryder, O. S., Yatavelli, R. L. N., Thornton, J. A., Cubison, M. J., Gonin, M., and  
462 Worsnop, D. R.: A field-deployable, chemical ionization time-of-flight mass spectrometer, *Atmos. Meas. Tech.*, 4, 1471-1479,  
463 10.5194/amt-4-1471-2011, 2011.

464 Bianchi, F., Kurtén, T., Riva, M., Mohr, C., Rissanen, M. P., Roldin, P., Berndt, T., Crouse, J. D., Wennberg, P. O., Mentel,  
465 T. F., Wildt, J., Junninen, H., Jokinen, T., Kulmala, M., Worsnop, D. R., Thornton, J. A., Donahue, N., Kjaergaard, H. G., and  
466 Ehn, M.: Highly Oxygenated Organic Molecules (HOM) from Gas-Phase Autoxidation Involving Peroxy Radicals: A Key  
467 Contributor to Atmospheric Aerosol, *Chem Rev*, 10.1021/acs.chemrev.8b00395, 2019.

468 Bonn, B., and Moortgat, G. K.: Sesquiterpene ozonolysis: Origin of atmospheric new particle formation from biogenic  
469 hydrocarbons, 30, doi:10.1029/2003GL017000, 2003.

470 Boy, M., Bonn, B., Maso, M. D., Hakola, H., Hirsikko, A., Kulmala, M., Kurtén, T., Laakso, L., Mäkelä, J., Riipinen, I.,  
471 Rannik, Ü., Sihto, S.-L., and Ruuskanen, T. M.: Biogenic Sesquiterpenes and Atmospheric New Particle Formation: A Boreal  
472 Forest Site Investigation, *Nucleation and Atmospheric Aerosols*, Dordrecht, 2007, 344-349,

473 Boyd, C. M., Sanchez, J., Xu, L., Eugene, A. J., Nah, T., Tuet, W. Y., Guzman, M. I., and Ng, N. L.: Secondary organic aerosol  
474 formation from the  $\beta$ -pinene +  $\text{NO}_3$  system: effect of humidity and peroxy radical fate, *Atmos. Chem. Phys.*, 15, 7497-7522,  
475 10.5194/acp-15-7497-2015, 2015.

476 Breitenlechner, M., Fischer, L., Hainer, M., Heinritzi, M., Curtius, J., and Hansel, A.: PTR3: An Instrument for Studying the  
477 Lifecycle of Reactive Organic Carbon in the Atmosphere, *Analytical Chemistry*, 89, 5824-5831,  
478 10.1021/acs.analchem.6b05110, 2017.

479 Bsaibes, S., Al Ajami, M., Mermet, K., Truong, F., Batut, S., Hecquet, C., Dusanter, S., Léonadis, T., Sauvage, S., Kammer,  
480 J., Flaud, P.-M., Perraudin, E., Villenave, E., Locoge, N., Gros, V., and Schoemaeker, C.: Variability of OH reactivity in the  
481 Landes maritime Pine forest: Results from the LANDEX campaign 2017, *Atmos. Chem. Phys. Discuss.*,  
482 <https://doi.org/10.5194/acp-2019-548>, in review, 2019.

483 Buhr, K., van Ruth, S., and Delahunty, C.: Analysis of volatile flavour compounds by Proton Transfer Reaction-Mass  
484 Spectrometry: fragmentation patterns and discrimination between isobaric and isomeric compounds, *International Journal of*  
485 *Mass Spectrometry*, 221, 1-7, [https://doi.org/10.1016/S1387-3806\(02\)00896-5](https://doi.org/10.1016/S1387-3806(02)00896-5), 2002.

486 Buser, A. M., Kierkegaard, A., Bogdal, C., MacLeod, M., Scheringer, M., and Hungerbühler, K.: Concentrations in Ambient  
487 Air and Emissions of Cyclic Volatile Methylsiloxanes in Zurich, Switzerland, *Environmental Science & Technology*, 47,  
488 7045-7051, 10.1021/es3046586, 2013.

489 Calfapietra, C., Fares, S., Manes, F., Morani, A., Sgrigna, G., and Loreto, F.: Role of Biogenic Volatile Organic Compounds  
490 (BVOC) emitted by urban trees on ozone concentration in cities: A review, *Environ Pollut*, 183, 71-80,  
491 <https://doi.org/10.1016/j.envpol.2013.03.012>, 2013.

492 Carlton, A. G., Wiedinmyer, C., and Kroll, J. H.: A review of Secondary Organic Aerosol (SOA) formation from isoprene,  
493 *Atmos. Chem. Phys.*, 9, 4987-5005, 10.5194/acp-9-4987-2009, 2009.

494 Carslaw, K. S., Lee, L. A., Reddington, C. L., Pringle, K. J., Rap, A., Forster, P. M., Mann, G. W., Spracklen, D. V.,  
495 Woodhouse, M. T., Regayre, L. A., and Pierce, J. R.: Large contribution of natural aerosols to uncertainty in indirect forcing,  
496 *Nature*, 503, 67, 10.1038/nature12674, 2013.

497 Claeys, M., Graham, B., Vas, G., Wang, W., Vermeylen, R., Pashynska, V., Cafmeyer, J., Guyon, P., Andreae, M. O., Artaxo,  
498 P., and Maenhaut, W.: Formation of Secondary Organic Aerosols Through Photooxidation of Isoprene, 303, 1173-1176,  
499 10.1126/science.1092805 %J Science, 2004.

500 Corchnoy, S. B., Arey, J., and Atkinson, R.: Hydrocarbon emissions from twelve urban shade trees of the Los Angeles,  
501 California, Air Basin, Atmospheric Environment. Part B. Urban Atmosphere, 26, 339-348, [https://doi.org/10.1016/0957-1272\(92\)90009-H](https://doi.org/10.1016/0957-1272(92)90009-H), 1992.

503 Criegee, R.: Mechanism of Ozonolysis, *Angewandte Chemie International Edition in English*, 14, 745-752,  
504 10.1002/anie.197507451, 1975.

505 Crounse, J. D., McKinney, K. A., Kwan, A. J., and Wennberg, P. O.: Measurement of Gas-Phase Hydroperoxides by Chemical  
506 Ionization Mass Spectrometry, *Analytical Chemistry*, 78, 6726-6732, 10.1021/ac0604235, 2006.

507 Donahue, N. M., Kroll, J. H., Pandis, S. N., and Robinson, A. L.: A two-dimensional volatility basis set – Part 2: Diagnostics  
508 of organic-aerosol evolution, *Atmos. Chem. Phys.*, 12, 615-634, 10.5194/acp-12-615-2012, 2012.

509 Dreyfus, G. B., Schade, G. W., and Goldstein, A. H.: Observational constraints on the contribution of isoprene oxidation to  
510 ozone production on the western slope of the Sierra Nevada, California, *Journal of Geophysical Research: Atmospheres*, 107,  
511 ACH 1-1-ACH 1-17, 10.1029/2001JD001490, 2002.

512 Dusanter, S., Vimal, D., and Stevens, P. S.: Technical note: Measuring tropospheric OH and HO<sub>2</sub> by laser-induced  
513 fluorescence at low pressure. A comparison of calibration techniques, *Atmos. Chem. Phys.*, 8, 321–340,  
514 <https://doi.org/10.5194/acp-8-321-2008>, 2008.

515 Ehn, M., Kleist, E., Junninen, H., Petäjä, T., Lönn, G., Schobesberger, S., Dal Maso, M., Trimborn, A., Kulmala, M., Worsnop,  
516 D. R., Wahner, A., Wildt, J., and Mentel, T. F.: Gas phase formation of extremely oxidized pinene reaction products in chamber  
517 and ambient air, *Atmos. Chem. Phys.*, 12, 5113-5127, 10.5194/acp-12-5113-2012, 2012.

518 Ehn, M., Thornton, J. A., Kleist, E., Sipila, M., Junninen, H., Pullinen, I., Springer, M., Rubach, F., Tillmann, R., Lee, B.,  
519 Lopez-Hilfiker, F., Andres, S., Acir, I. H., Rissanen, M., Jokinen, T., Schobesberger, S., Kangasluoma, J., Kontkanen, J.,  
520 Nieminen, T., Kurten, T., Nielsen, L. B., Jorgensen, S., Kjaergaard, H. G., Canagaratna, M., Dal Maso, M., Berndt, T., Petaja,  
521 T., Wahner, A., Kerminen, V. M., Kulmala, M., Worsnop, D. R., Wildt, J., and Mentel, T. F.: A large source of low-volatility  
522 secondary organic aerosol, *Nature*, 506, 476–+, 2014.

523 Gill, K. J., and Hites, R. A.: Rate Constants for the Gas-Phase Reactions of the Hydroxyl Radical with Isoprene,  $\alpha$ - and  $\beta$ -  
524 Pinene, and Limonene as a Function of Temperature, *The Journal of Physical Chemistry A*, 106, 2538-2544,  
525 10.1021/jp013532q, 2002.

526

527 Goldstein, A. H., McKay, M., Kurpius, M. R., Schade, G. W., Lee, A., Holzinger, R., and Rasmussen, R. A.: Forest thinning  
528 experiment confirms ozone deposition to forest canopy is dominated by reaction with biogenic VOCs, *Geophys Res Lett*, 31,  
529 10.1029/2004GL021259, 2004.

530 Gueneron, M., Erickson, M. H., VanderSchelden, G. S., and Jobson, B. T.: PTR-MS fragmentation patterns of gasoline  
531 hydrocarbons, *International Journal of Mass Spectrometry*, 379, 97-109, <https://doi.org/10.1016/j.ijms.2015.01.001>, 2015.

532 Guenther, A., Hewitt, C. N., Erickson, D., Fall, R., Geron, C., Graedel, T., Harley, P., Klinger, L., Lerdau, M., McKay, W. A.,  
533 Pierce, T., Scholes, B., Steinbrecher, R., Tallamraju, R., Taylor, J., and Zimmerman, P.: A global model of natural volatile  
534 organic compound emissions, *Journal of Geophysical Research: Atmospheres*, 100, 8873-8892, 10.1029/94JD02950, 1995.

535 Hakola, H., Tarvainen, V., Bäck, J., Ranta, H., Bonn, B., Rinne, J., and Kulmala, M.: Seasonal variation of mono- and  
536 sesquiterpene emission rates of Scots pine, *Biogeosciences*, 3, 93-101, 10.5194/bg-3-93-2006, 2006.

537 Hakola, H., Hellén, H., Hemmilä, M., Rinne, J., and Kulmala, M.: In situ measurements of volatile organic compounds in a  
538 boreal forest, *Atmos. Chem. Phys.*, 12, 11665-11678, 10.5194/acp-12-11665-2012, 2012.

539 Hallquist, M., Wängberg, I., Ljungström, E., Barnes, I., and Becker, K.-H.: Aerosol and Product Yields from NO<sub>3</sub> Radical-  
540 Initiated Oxidation of Selected Monoterpenes, *Environmental Science & Technology*, 33, 553-559, 10.1021/es980292s, 1999.

541 Hatfield, M. L., and Huff Hartz, K. E.: Secondary organic aerosol from biogenic volatile organic compound mixtures, *Atmos  
542 Environ*, 45, 2211-2219, <https://doi.org/10.1016/j.atmosenv.2011.01.065>, 2011.

543 Hellén, H., Hakola, H., Pystynen, K.-H., Rinne, J., and Haapanala, S.: C<sub>2</sub>-C<sub>10</sub> hydrocarbon emissions from a boreal wetland  
544 and forest floor, *Biogeosciences*, 3, 167–174, <https://doi.org/10.5194/bg-3-167-2006>, 2006.

545 Hellén, H., Praplan, A. P., Tykkä, T., Ylivinkka, I., Vakkari, V., Bäck, J., Petäjä, T., Kulmala, M., and Hakola, H.: Long-term  
546 measurements of volatile organic compounds highlight the importance of sesquiterpenes for the atmospheric chemistry of a  
547 boreal forest, *Atmos. Chem. Phys.*, 18, 13839-13863, 10.5194/acp-18-13839-2018, 2018.

548 Henze, D. K., and Seinfeld, J. H.: Global secondary organic aerosol from isoprene oxidation, *Geophys Res Lett*, 33,  
549 10.1029/2006GL025976, 2006.

550 Holzinger, R., Acton, W. J. F., Bloss, W. J., Breitenlechner, M., Crilley, L. R., Dusanter, S., Gonin, M., Gros, V., Keutsch, F.  
551 N., Kiendler-Scharr, A., Kramer, L. J., Krechmer, J. E., Languille, B., Locoge, N., Lopez-Hilfiker, F., Materić, D., Moreno,  
552 S., Nemitz, E., Quéléver, L. L. J., Sarda Esteve, R., Sauvage, S., Schallhart, S., Sommariva, R., Tillmann, R., Wedel, S.,  
553 Worton, D. R., Xu, K., and Zaytsev, A.: Validity and limitations of simple reaction kinetics to calculate concentrations of  
554 organic compounds from ion counts in PTR-MS, *Atmos. Meas. Tech.*, 12, 6193–6208, [https://doi.org/10.5194/amt-12-6193-](https://doi.org/10.5194/amt-12-6193-2019)  
555 2019, 2019.

556 Hyttinen, N., Kupiainen-Määttä, O., Rissanen, M. P., Muuronen, M., Ehn, M., and Kurtén, T.: Modeling the Charging of  
557 Highly Oxidized Cyclohexene Ozonolysis Products Using Nitrate-Based Chemical Ionization, *The Journal of Physical*  
558 *Chemistry A*, 119, 6339–6345, 10.1021/acs.jpca.5b01818, 2015.

559 Intergovernmental Panel on Climate Change (IPCC), *Climate Change 2013: The Physical Science Basis. Contribution of*  
560 *Working Group I to the Fifth Assessment Report of the Intergovernmental Panel on Climate Change*, 1535 pp., Cambridge  
561 Univ. Press, Cambridge, U. K., and New York, 2013.

562 Isaacman-VanWertz, G., Massoli, P., O'Brien, R., Lim, C., Franklin, J. P., Moss, J. A., Hunter, J. F., Nowak, J. B., Canagaratna,  
563 M. R., Misztal, P. K., Arata, C., Roscioli, J. R., Herndon, S. T., Onasch, T. B., Lambe, A. T., Jayne, J. T., Su, L. P., Knopf, D.  
564 A., Goldstein, A. H., Worsnop, D. R., and Kroll, J. H.: Chemical evolution of atmospheric organic carbon over multiple  
565 generations of oxidation, *Nat Chem*, 10, 462–468, 2018.

566 Jardine, K., Yañez Serrano, A., Arneth, A., Abrell, L., Jardine, A., van Haren, J., Artaxo, P., Rizzo, L. V., Ishida, F. Y., Karl,  
567 T., Kesselmeier, J., Saleska, S., and Huxman, T.: Within-canopy sesquiterpene ozonolysis in Amazonia, 116,  
568 doi:10.1029/2011JD016243, 2011.

569 Jimenez, J. L., Canagaratna, M. R., Donahue, N. M., Prevot, A. S. H., Zhang, Q., Kroll, J. H., DeCarlo, P. F., Allan, J. D., Coe,  
570 H., Ng, N. L., Aiken, A. C., Docherty, K. S., Ulbrich, I. M., Grieshop, A. P., Robinson, A. L., Duplissy, J., Smith, J. D., Wilson,  
571 K. R., Lanz, V. A., Hueglin, C., Sun, Y. L., Tian, J., Laaksonen, A., Raatikainen, T., Rautiainen, J., Vaattovaara, P., Ehn, M.,  
572 Kulmala, M., Tomlinson, J. M., Collins, D. R., Cubison, M. J., Dunlea, J., Huffman, J. A., Onasch, T. B., Alfarra, M. R.,  
573 Williams, P. I., Bower, K., Kondo, Y., Schneider, J., Drewnick, F., Borrmann, S., Weimer, S., Demerjian, K., Salcedo, D.,  
574 Cottrell, L., Griffin, R., Takami, A., Miyoshi, T., Hatakeyama, S., Shimojo, A., Sun, J. Y., Zhang, Y. M., Dzepina, K., Kimmel,  
575 J. R., Sueper, D., Jayne, J. T., Herndon, S. C., Trimborn, A. M., Williams, L. R., Wood, E. C., Middlebrook, A. M., Kolb, C.  
576 E., Baltensperger, U., and Worsnop, D. R.: Evolution of Organic Aerosols in the Atmosphere, 326, 1525–1529,  
577 10.1126/science.1180353 %J Science, 2009.

578 Jokinen, T., Sipilä, M., Richters, S., Kerminen, V.-M., Paasonen, P., Stratmann, F., Worsnop, D., Kulmala, M., Ehn, M.,  
579 Herrmann, H., and Berndt, T.: Rapid Autoxidation Forms Highly Oxidized RO<sub>2</sub> Radicals in the Atmosphere, 53, 14596–14600,  
580 doi:10.1002/anie.201408566, 2014.

581 Jokinen, T., Berndt, T., Makkonen, R., Kerminen, V.-M., Junninen, H., Paasonen, P., Stratmann, F., Herrmann, H., Guenther,  
582 A. B., Worsnop, D. R., Kulmala, M., Ehn, M., and Sipilä, M.: Production of extremely low volatile organic compounds from  
583 biogenic emissions: Measured yields and atmospheric implications, 112, 7123–7128, 10.1073/pnas.1423977112 %J  
584 *Proceedings of the National Academy of Sciences*, 2015.

585 Kammer, J., Perraudin, E., Flaud, P. M., Lamaud, E., Bonnefond, J. M., and Villenave, E.: Observation of nighttime new  
586 particle formation over the French Landes forest, *Sci Total Environ*, 621, 1084–1092,  
587 <https://doi.org/10.1016/j.scitotenv.2017.10.118>, 2018.

588 Kanakidou, M., Seinfeld, J. H., Pandis, S. N., Barnes, I., Dentener, F. J., Facchini, M. C., Van Dingenen, R., Ervens, B., Nenes,  
589 A., Nielsen, C. J., Swietlicki, E., Putaud, J. P., Balkanski, Y., Fuzzi, S., Horth, J., Moortgat, G. K., Winterhalter, R., Myhre,  
590 C. E. L., Tsigaridis, K., Vignati, E., Stephanou, E. G., and Wilson, J.: Organic aerosol and global climate modelling: a review,  
591 *Atmos. Chem. Phys.*, 5, 1053–1123, <https://doi.org/10.5194/acp-5-1053-2005>, 2005.

592 Kanawade, V. P., Jobson, B. T., Guenther, A. B., Erupe, M. E., Pressley, S. N., Tripathi, S. N., and Lee, S. H.: Isoprene  
593 suppression of new particle formation in a mixed deciduous forest, *Atmos. Chem. Phys.*, 11, 6013–6027, 10.5194/acp-11-  
594 6013-2011, 2011.

595 Karl, M., Brauers, T., Dorn, H. P., Holland, F., Komenda, M., Poppe, D., Rohrer, F., Rupp, L., Schaub, A., and Wahner, A.:  
596 Kinetic Study of the OH-isoprene and O<sub>3</sub>-isoprene reaction in the atmosphere simulation chamber, SAPHIR, *Geophys Res*  
597 *Lett*, 31, 10.1029/2003GL019189, 2004.

598 Karl, T., Hansel, A., Cappellin, L., Kaser, L., Herdlinger-Blatt, I., and Jud, W.: Selective measurements of isoprene and 2-  
599 methyl-3-buten-2-ol based on NO<sup>+</sup> ionization mass spectrometry, *Atmos. Chem. Phys.*, 12, 11877–11884,  
600 <https://doi.org/10.5194/acp-12-11877-2012>, 2012.

601 Kari, E., Miettinen, P., Yli-Pirilä, P., Virtanen, A., and Faiola, C. L.: PTR-ToF-MS product ion distributions and humidity-  
602 dependence of biogenic volatile organic compounds, *International Journal of Mass Spectrometry*, 430, 87-97,  
603 <https://doi.org/10.1016/j.ijms.2018.05.003>, 2018.

604 Kaser, L., Karl, T., Guenther, A., Graus, M., Schnitzhofer, R., Turnipseed, A., Fischer, L., Harley, P., Madronich, M., Gochis,  
605 D., Keutsch, F. N., and Hansel, A.: Undisturbed and disturbed above canopy ponderosa pine emissions: PTR-TOF-MS  
606 measurements and MEGAN 2.1 model results, *Atmos. Chem. Phys.*, 13, 11935–11947, [https://doi.org/10.5194/acp-13-11935-](https://doi.org/10.5194/acp-13-11935-2013)  
607 2013, 2013.

608 Keck, L., Hoeschen, C., and Oeh, U.: Effects of carbon dioxide in breath gas on proton transfer reaction-mass spectrometry  
609 (PTR-MS) measurements, *International Journal of Mass Spectrometry*, 270, 156-165,  
610 <https://doi.org/10.1016/j.ijms.2007.12.009>, 2008.

611 Keeling, C. I., and Bohmann, J.: Diterpene resin acids in conifers, *Phytochemistry*, 67, 2415-2423,  
612 <https://doi.org/10.1016/j.phytochem.2006.08.019>, 2006.

613 Kesselmeier, J., and Staudt, M.: Biogenic Volatile Organic Compounds (VOC): An Overview on Emission, Physiology and  
614 Ecology, *J Atmos Chem*, 33, 23-88, 10.1023/A:1006127516791, 1999.

615 Khamaganov, V. G., and Hites, R. A.: Rate Constants for the Gas-Phase Reactions of Ozone with Isoprene,  $\alpha$ - and  $\beta$ -Pinene,  
616 and Limonene as a Function of Temperature, *The Journal of Physical Chemistry A*, 105, 815-822, 10.1021/jp002730z, 2001.

617 Khan, M. A. H., Ashfold, M. J., Nickless, G., Martin, D., Watson, L. A., Hamer, P. D., Wayne, R. P., Canosa-Mas, C. E., and  
618 Shallcross, D. E.: Night-time NO<sub>3</sub> and OH radical concentrations in the United Kingdom inferred from hydrocarbon  
619 measurements, *Atmospheric Science Letters*, 9, 140-146, 10.1002/asl.175, 2008.

620 Kiendler-Scharr, A., Wildt, J., Maso, M. D., Hohaus, T., Kleist, E., Mentel, T. F., Tillmann, R., Uerlings, R., Schurr, U., and  
621 Wahner, A.: New particle formation in forests inhibited by isoprene emissions, *Nature*, 461, 381, 10.1038/nature08292  
622 <https://www.nature.com/articles/nature08292#supplementary-information>, 2009.

623 Kiendler-Scharr, A., Mensah, A. A., Friese, E., Topping, D., Nemitz, E., Prevot, A. S. H., Äijälä, M., Allan, J., Canonaco, F.,  
624 Canagaratna, M., Carbone, S., Crippa, M., Dall'Osto, M., Day, D. A., De Carlo, P., Di Marco, C. F., Elbern, H., Eriksson, A.,  
625 Freney, E., Hao, L., Herrmann, H., Hildebrandt, L., Hillamo, R., Jimenez, J. L., Laaksonen, A., McFiggans, G., Mohr, C.,  
626 O'Dowd, C., Otjes, R., Ovadnevaite, J., Pandis, S. N., Poulain, L., Schlag, P., Sellegri, K., Swietlicki, E., Tiitta, P., Vermeulen,  
627 A., Wahner, A., Worsnop, D., and Wu, H. C.: Ubiquity of organic nitrates from nighttime chemistry in the European submicron  
628 aerosol, *Geophys Res Lett*, 43, 7735-7744, 10.1002/2016GL069239, 2016.

629 Kim, S., Karl, T., Helmig, D., Daly, R., Rasmussen, R., and Guenther, A.: Measurement of atmospheric sesquiterpenes by  
630 proton transfer reaction-mass spectrometry (PTR-MS), *Atmos. Meas. Tech.*, 2, 99-112, 10.5194/amt-2-99-2009, 2009.

631 Kirkby, J., Duplissy, J., Sengupta, K., Frege, C., Gordon, H., Williamson, C., Heinritzi, M., Simon, M., Yan, C., Almeida, J.,  
632 Tröstl, J., Nieminen, T., Ortega, I. K., Wagner, R., Adamov, A., Amorim, A., Bernhammer, A.-K., Bianchi, F., Breitenlechner,  
633 M., Brilke, S., Chen, X., Craven, J., Dias, A., Ehrhart, S., Flagan, R. C., Franchin, A., Fuchs, C., Guida, R., Hakala, J., Hoyle,  
634 C. R., Jokinen, T., Junninen, H., Kangasluoma, J., Kim, J., Krapf, M., Kürten, A., Laaksonen, A., Lehtipalo, K., Makhmutov,  
635 V., Mathot, S., Molteni, U., Onnela, A., Peräkylä, O., Piel, F., Petäjä, T., Praplan, A. P., Pringle, K., Rap, A., Richards, N. A.  
636 D., Riipinen, I., Rissanen, M. P., Rondo, L., Sarnela, N., Schobesberger, S., Scott, C. E., Seinfeld, J. H., Sipilä, M., Steiner,  
637 G., Stozhkov, Y., Stratmann, F., Tomé, A., Virtanen, A., Vogel, A. L., Wagner, A. C., Wagner, P. E., Weingartner, E., Wimmer,  
638 D., Winkler, P. M., Ye, P., Zhang, X., Hansel, A., Dommen, J., Donahue, N. M., Worsnop, D. R., Baltensperger, U., Kulmala,  
639 M., Carslaw, K. S., and Curtius, J.: Ion-induced nucleation of pure biogenic particles, *Nature*, 533, 521, 10.1038/nature17953,  
640 2016.

641 Krechmer, J., Lopez-Hilfiker, F., Koss, A., Hutterli, M., Stoermer, C., Deming, B., Kimmel, J., Warneke, C., Holzinger, R.,  
642 Jayne, J., Worsnop, D., Fuhrer, K., Gonin, M., and de Gouw, J.: Evaluation of a New Reagent-Ion Source and Focusing Ion-  
643 Molecule Reactor for Use in Proton-Transfer-Reaction Mass Spectrometry, *Analytical Chemistry*, 90, 12011-12018,  
644 10.1021/acs.analchem.8b02641, 2018.

645 Lavy, M., Zuker, A., Lewinsohn, E., Larkov, O., Ravid, U., Vainstein, A., and Weiss, D.: Linalool and linalool oxide  
646 production in transgenic carnation flowers expressing the *Clarkia breweri* linalool synthase gene, *Molecular Breeding*, 9, 103-  
647 111, 10.1023/A:1026755414773, 2002.

648 Lee, B. H., Lopez-Hilfiker, F. D., Mohr, C., Kurten, T., Worsnop, D. R., and Thornton, J. A.: An Iodide-Adduct High-  
649 Resolution Time-of-Flight Chemical-Ionization Mass Spectrometer: Application to Atmospheric Inorganic and Organic  
650 Compounds, *Environmental Science & Technology*, 48, 6309-6317, 2014.

651 Lide, D. R. *CRC Handbook of Chemistry and Physics; Internet Version 2005*, <<http://www.hbcpnetbase.com>>, CRC Press,  
652 Boca Raton, FL, 2005.

653 Liu, X., Deming, B., Pagonis, D., Day, D. A., Palm, B. B., Talukdar, R., Roberts, J. M., Veres, P. R., Krechmer, J. E., Thornton,  
654 J. A., de Gouw, J. A., Ziemann, P. J., and Jimenez, J. L.: Effects of Gas-Wall Interactions on Measurements of Semivolatile  
655 Compounds and Small Polar Molecules, *Atmos. Meas. Tech. Discuss.*, <https://doi.org/10.5194/amt-2019-52>, in review, 2019.

656 Maleknia, S. D., Bell, T. L., and Adams, M. A.: PTR-MS analysis of reference and plant-emitted volatile organic compounds,  
657 *International Journal of Mass Spectrometry*, 262, 203-210, <https://doi.org/10.1016/j.ijms.2006.11.010>, 2007.

658 Maria, S. F., Russell, L. M., Gilles, M. K., and Myneni, S. C. B.: Organic Aerosol Growth Mechanisms and Their Climate-  
659 Forcing Implications, 306, 1921-1924, 10.1126/science.1103491 %J Science, 2004.

660 Massoli, P., Stark, H., Canagaratna, M. R., Krechmer, J. E., Xu, L., Ng, N. L., Mauldin, R. L., Yan, C., Kimmel, J., Misztal,  
661 P. K., Jimenez, J. L., Jayne, J. T., and Worsnop, D. R.: Ambient Measurements of Highly Oxidized Gas-Phase Molecules  
662 during the Southern Oxidant and Aerosol Study (SOAS) 2013, *ACS Earth and Space Chemistry*, 2, 653-672,  
663 10.1021/acsearthspacechem.8b00028, 2018.

664 Matsunaga, S. N., Chatani, S., Nakatsuka, S., Kusumoto, D., Kubota, K., Utsumi, Y., Enoki, T., Tani, A., and Hiura, T.:  
665 Determination and potential importance of diterpene (kaur-16-ene) emitted from dominant coniferous trees in Japan,  
666 *Chemosphere*, 87, 886-893, <https://doi.org/10.1016/j.chemosphere.2012.01.040>, 2012.

667 Mauderly, J. L., and Chow, J. C.: Health Effects of Organic Aerosols, *Inhalation Toxicology*, 20, 257-288,  
668 10.1080/08958370701866008, 2008.

669 McFiggans, G., Mentel, T. F., Wildt, J., Pullinen, I., Kang, S., Kleist, E., Schmitt, S., Springer, M., Tillmann, R., Wu, C., Zhao,  
670 D., Hallquist, M., Faxon, C., Le Breton, M., Hallquist, Å. M., Simpson, D., Bergström, R., Jenkin, M. E., Ehn, M., Thornton,  
671 J. A., Alfarra, M. R., Bannan, T. J., Percival, C. J., Priestley, M., Topping, D., and Kiendler-Scharr, A.: Secondary organic  
672 aerosol reduced by mixture of atmospheric vapours, *Nature*, 565, 587-593, 10.1038/s41586-018-0871-y, 2019.

673 Mermet, K., Sauvage, S., Dusanter, S., Salameh, T., Léonardis, T., Flaud, P.-M., Perraudin, É., Villenave, É., and Locoge, N.:  
674 Optimization of a gas chromatographic unit for measuring BVOCs in ambient air, *Atmos. Meas. Tech. Discuss.*,  
675 <https://doi.org/10.5194/amt-2019-224>, in review, 2019.

676 Monson, R. K., and Fall, R.: Isoprene Emission from Aspen Leaves, Influence of Environment and Relation to Photosynthesis  
677 and Photorespiration, 90, 267-274, 10.1104/pp.90.1.267 %J Plant Physiology, 1989.

678 Moreaux, V., Lamaud, É., Bosc, A., Bonnefond, J.-M., Medlyn, B. E., and Loustau, D.: Paired comparison of water, energy  
679 and carbon exchanges over two young maritime pine stands (*Pinus pinaster* Ait.): effects of thinning and weeding in the early  
680 stage of tree growth, *Tree Physiology*, 31, 903-921, 10.1093/treephys/tpr048, 2011.

681 Ng, N. L., Brown, S. S., Archibald, A. T., Atlas, E., Cohen, R. C., Crowley, J. N., Day, D. A., Donahue, N. M., Fry, J. L.,  
682 Fuchs, H., Griffin, R. J., Guzman, M. I., Herrmann, H., Hodzic, A., Iinuma, Y., Jimenez, J. L., Kiendler-Scharr, A., Lee, B.  
683 H., Luecken, D. J., Mao, J., McLaren, R., Mutzel, A., Osthoff, H. D., Ouyang, B., Picquet-Varrault, B., Platt, U., Pye, H. O.  
684 T., Rudich, Y., Schwantes, R. H., Shiraiwa, M., Stutz, J., Thornton, J. A., Tilgner, A., Williams, B. J., and Zaveri, R. A.:  
685 Nitrate radicals and biogenic volatile organic compounds: oxidation, mechanisms, and organic aerosol, *Atmos. Chem. Phys.*,  
686 17, 2103-2162, 10.5194/acp-17-2103-2017, 2017.

687 Peräkylä, O., Vogt, M., Tikkanen, O.-P., Laurila, T., Kajos, M. K., Rantala, P. A., Patokoski, J., Aalto, J., Yli-Juuti, T., Ehn,  
688 M., Sipilä, M., Paasonen, P., Rissanen, M., Nieminen, T., Taipale, R., Keronen, P., Lappalainen, H. K., Ruuskanen, T. M.,  
689 Rinne, J., Kerminen, V.-M., Kulmala, M., Bäck, J., and Petäjä, T.: Monoterpenes' oxidation capacity and rate over a boreal  
690 forest: temporal variation and connection to growth of newly formed particles, *Boreal Environ. Res.*, 19, 293-310, 2014.

691 Petäjä, T., Mauldin, I. R. L., Kosciuch, E., McGrath, J., Nieminen, T., Paasonen, P., Boy, M., Adamov, A., Kotiaho, T., and  
692 Kulmala, M.: Sulfuric acid and OH concentrations in a boreal forest site, *Atmos. Chem. Phys.*, 9, 7435-7448, 10.5194/acp-9-  
693 7435-2009, 2009.

694 Pfeiffer, T., Forberich, O., and Comes, F. J.: The contribution of the ozonolysis of terpenes to tropospheric OH concentrations,  
695 *Canadian Journal of Physics*, 79, 131-142, 10.1139/p01-030, 2001.



696 Presto, A. A., Huff Hartz, K. E., and Donahue, N. M.: Secondary Organic Aerosol Production from Terpene Ozonolysis. 2.  
697 Effect of NO<sub>x</sub> Concentration, *Environmental Science & Technology*, 39, 7046-7054, 10.1021/es050400s, 2005.

698 Qin, M., Hu, Y., Wang, X., Vasilakos, P., Boyd, C. M., Xu, L., Song, Y., Ng, N. L., Nenes, A., and Russell, A. G.: Modeling  
699 biogenic secondary organic aerosol (BSOA) formation from monoterpene reactions with NO<sub>3</sub>: A case study of the SOAS  
700 campaign using CMAQ, *Atmos Environ*, 184, 146-155, <https://doi.org/10.1016/j.atmosenv.2018.03.042>, 2018.

701 Ren, X., Harder, H., Martinez, M., Leshner, R. L., Oligier, A., Shirley, T., Adams, J., Simpas, J. B., and Brune, W. H.: HO<sub>x</sub>  
702 concentrations and OH reactivity observations in New York City during PMTACS-NY2001, *Atmos Environ*, 37, 3627-3637,  
703 [https://doi.org/10.1016/S1352-2310\(03\)00460-6](https://doi.org/10.1016/S1352-2310(03)00460-6), 2003.

704 Rickard, A. R., Johnson, D., McGill, C. D., and Marston, G.: OH yields in the gas-phase reactions of ozone with alkenes, *J*  
705 *Phys Chem A*, 103, 7656-7664, 1999.

706 Riva, M., Rantala, P., Krechmer, J. E., Peräkylä, O., Zhang, Y., Heikkinen, L., Garmash, O., Yan, C., Kulmala, M., Worsnop,  
707 D., and Ehn, M.: Evaluating the performance of five different chemical ionization techniques for detecting gaseous oxygenated  
708 organic species, *Atmos. Meas. Tech.*, 12, 2403-2421, <https://doi.org/10.5194/amt-12-2403-2019>, 2019a.

709 Riva, M., Heikkinen, L., Bell, D. M., Peräkylä, O., Zha, Q., Schallhart, S., Rissanen, M. P., Imre, D., Petäjä, T., Thornton, J.  
710 A., Zelenyuk, A., and Ehn, M.: Chemical transformations in monoterpene-derived organic aerosol enhanced by inorganic  
711 composition, *npj Climate and Atmospheric Science*, 2, 2, 10.1038/s41612-018-0058-0, 2019b.

712 Ruppert, L., and Heinz Becker, K.: A product study of the OH radical-initiated oxidation of isoprene: formation of C<sub>5</sub>-  
713 unsaturated diols, *Atmos Environ*, 34, 1529-1542, [https://doi.org/10.1016/S1352-2310\(99\)00408-2](https://doi.org/10.1016/S1352-2310(99)00408-2), 2000.

714 Sakulyanontvittaya, T., Duhl, T., Wiedinmyer, C., Helmig, D., Matsunaga, S., Potosnak, M., Milford, J., and Guenther, A.:  
715 Monoterpene and Sesquiterpene Emission Estimates for the United States, *Environmental Science & Technology*, 42, 1623-  
716 1629, 10.1021/es702274e, 2008.

717

718 Schwarz, K., Filipiak, W., and Amann, A.: Determining concentration patterns of volatile compounds in exhaled breath by  
719 PTR-MS, *Journal of Breath Research*, 3, 027002, 10.1088/1752-7155/3/2/027002, 2009.

720 Sekimoto, K., Li, S.-M., Yuan, B., Koss, A., Coggon, M., Warneke, C., and de Gouw, J.: Calculation of the sensitivity of  
721 proton-transfer-reaction mass spectrometry (PTR-MS) for organic trace gases using molecular properties, *International Journal*  
722 *of Mass Spectrometry*, 421, 71-94, <https://doi.org/10.1016/j.ijms.2017.04.006>, 2017.

723 Shirinzadeh, B., Wang, C. C., and Deng, D. Q.: Diurnal variation of the OH concentration in ambient air, *Geophys Res Lett*,  
724 14, 123-126, 10.1029/GL014i002p00123, 1987.

725 Simon, V., Clement, B., Riba, M. - L., and Torres, L.: The Landes experiment: Monoterpenes emitted from the maritime pine,  
726 *J. Geophys. Res.*, 99( D8), 16501 - 16510, doi:10.1029/94JD00785, 1994.

727 Sindelarova, K., Granier, C., Bouarar, I., Guenther, A., Tilmes, S., Stavrou, T., Müller, J. F., Kuhn, U., Stefani, P., and  
728 Knorr, W.: Global data set of biogenic VOC emissions calculated by the MEGAN model over the last 30 years, *Atmos. Chem.*  
729 *Phys.*, 14, 9317-9341, 10.5194/acp-14-9317-2014, 2014.

730 Stone, D., Whalley, L. K., and Heard, D. E.: Tropospheric OH and HO<sub>2</sub> radicals: field measurements and model comparisons,  
731 *Chemical Society Reviews*, 41, 6348-6404, 10.1039/C2CS35140D, 2012.

732 Surratt, J. D., Chan, A. W. H., Eddingsaas, N. C., Chan, M., Loza, C. L., Kwan, A. J., Hersey, S. P., Flagan, R. C., Wennberg,  
733 P. O., and Seinfeld, J. H.: Reactive intermediates revealed in secondary organic aerosol formation from isoprene, 107, 6640-  
734 6645, 10.1073/pnas.0911114107 %J Proceedings of the National Academy of Sciences, 2010.

735 Tani, A., Hayward, S., and Hewitt, C. N.: Measurement of monoterpenes and related compounds by proton transfer reaction-  
736 mass spectrometry (PTR-MS), *International Journal of Mass Spectrometry*, 223-224, 561-578, [https://doi.org/10.1016/S1387-3806\(02\)00880-1](https://doi.org/10.1016/S1387-3806(02)00880-1), 2003.

737

738 Tani, A., Hayward, S., Hansel, A., and Hewitt, C. N.: Effect of water vapour pressure on monoterpene measurements using  
739 proton transfer reaction-mass spectrometry (PTR-MS), *International Journal of Mass Spectrometry*, 239, 161-169,  
740 <https://doi.org/10.1016/j.ijms.2004.07.020>, 2004.

741 Tani, A.: Fragmentation and Reaction Rate Constants of Terpenoids Determined by Proton Transfer Reaction-mass  
742 Spectrometry, *Environmental Control in Biology*, 51, 23-29, 10.2525/ecb.51.23, 2013.

743 Tsigaridis, K., and Kanakidou, M.: Global modelling of secondary organic aerosol in the troposphere: a sensitivity analysis,  
744 *Atmos. Chem. Phys.*, 3, 1849-1869, 10.5194/acp-3-1849-2003, 2003.

745 von Schwartzberg, K., Schultze, W., and Kassner, H. J. P. C. R.: The moss *Physcomitrella patens* releases a tetracyclic  
746 diterpene, 22, 780-786, 10.1007/s00299-004-0754-6, 2004.

747 Warneke, C., de Gouw, J. A., Kuster, W. C., Goldan, P. D., and Fall, R.: Validation of Atmospheric VOC Measurements by  
748 Proton-Transfer- Reaction Mass Spectrometry Using a Gas-Chromatographic Preseparation Method, *Environmental Science  
749 & Technology*, 37, 2494-2501, 10.1021/es026266i, 2003.

750 Wei, D., Fuentes, J. D., Gerken, T., Chamecki, M., Trowbridge, A. M., Stoy, P. C., Katul, G. G., Fisch, G., Acevedo, O.,  
751 Manzi, A., von Randow, C., and dos Santos, R. M. N.: Environmental and biological controls on seasonal patterns of isoprene  
752 above a rain forest in central Amazonia, *Agricultural and Forest Meteorology*, 256-257, 391-406,  
753 <https://doi.org/10.1016/j.agrformet.2018.03.024>, 2018.

754 Wennberg, P. O., Bates, K. H., Crouse, J. D., Dodson, L. G., McVay, R. C., Mertens, L. A., Nguyen, T. B., Praske, E.,  
755 Schwantes, R. H., Smarte, M. D., St Clair, J. M., Teng, A. P., Zhang, X., and Seinfeld, J. H.: Gas-Phase Reactions of Isoprene  
756 and Its Major Oxidation Products, *Chem Rev*, 118, 3337-3390, 2018.

757 Winterhalter, R., Herrmann, F., Kanawati, B., Nguyen, T. L., Peeters, J., Vereecken, L., and Moortgat, G. K.: The gas-phase  
758 ozonolysis of  $\beta$ -caryophyllene (C<sub>15</sub>H<sub>24</sub>). Part I: an experimental study, *Physical Chemistry Chemical Physics*, 11, 4152-4172,  
759 10.1039/B817824K, 2009.

760 Xiong, F., McAvey, K. M., Pratt, K. A., Groff, C. J., Hostetler, M. A., Lipton, M. A., Starn, T. K., Seeley, J. V., Bertman, S.  
761 B., Teng, A. P., Crouse, J. D., Nguyen, T. B., Wennberg, P. O., Misztal, P. K., Goldstein, A. H., Guenther, A. B., Koss, A.  
762 R., Olson, K. F., de Gouw, J. A., Baumann, K., Edgerton, E. S., Feiner, P. A., Zhang, L., Miller, D. O., Brune, W. H., and  
763 Shepson, P. B.: Observation of isoprene hydroxynitrates in the southeastern United States and implications for the fate of NO<sub>x</sub>,  
764 *Atmos. Chem. Phys.*, 15, 11257-11272, <https://doi.org/10.5194/acp-15-11257-2015>, 2015.

765 Xu, L., Pye, H. O. T., He, J., Chen, Y., Murphy, B. N., and Ng, N. L.: Experimental and model estimates of the contributions  
766 from biogenic monoterpenes and sesquiterpenes to secondary organic aerosol in the southeastern United States, *Atmos. Chem.  
767 Phys.*, 18, 12613-12637, <https://doi.org/10.5194/acp-18-12613-2018>, 2018.

768 Yan, C., Nie, W., Äijälä, M., Rissanen, M. P., Canagaratna, M. R., Massoli, P., Junninen, H., Jokinen, T., Sarnela, N., Häme,  
769 S. A. K., Schobesberger, S., Canonaco, F., Yao, L., Prévôt, A. S. H., Petäjä, T., Kulmala, M., Sipilä, M., Worsnop, D. R., and  
770 Ehn, M.: Source characterization of highly oxidized multifunctional compounds in a boreal forest environment using positive  
771 matrix factorization, *Atmos. Chem. Phys.*, 16, 12715-12731, 10.5194/acp-16-12715-2016, 2016.

772 Yáñez-Serrano, A. M., Nölscher, A. C., Bourtsoukidis, E., Gomes Alves, E., Ganzeveld, L., Bonn, B., Wolff, S., Sa, M.,  
773 Yamasoe, M., Williams, J., Andreae, M. O., and Kesselmeier, J.: Monoterpene chemical speciation in a tropical  
774 rainforest: variation with season, height, and time of day at the Amazon Tall Tower Observatory (ATTO), *Atmos. Chem. Phys.*,  
775 18, 3403-3418, 10.5194/acp-18-3403-2018, 2018.

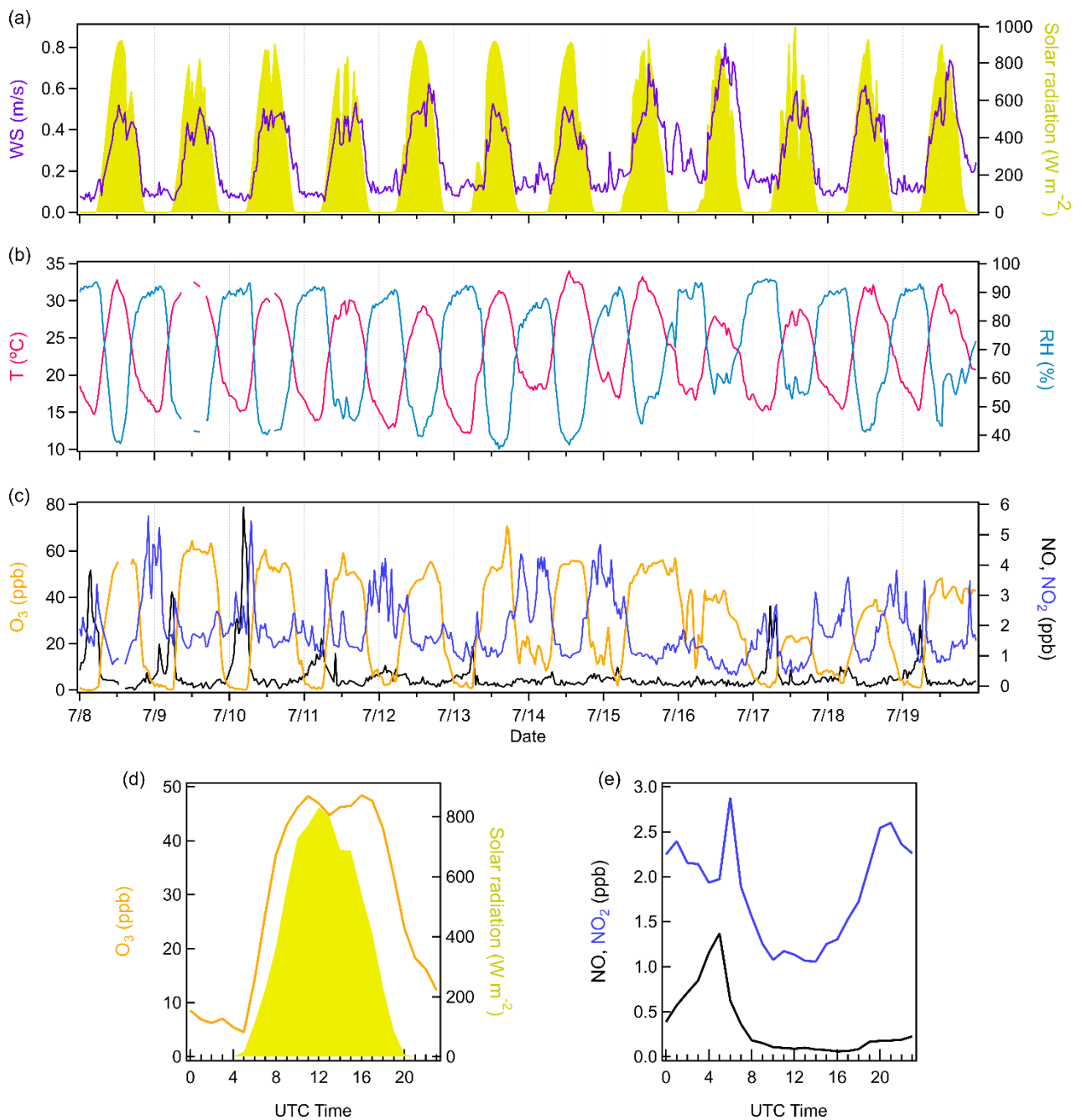
776 Yuan, B., Koss, A. R., Warneke, C., Coggon, M., Sekimoto, K., and de Gouw, J. A.: Proton-Transfer-Reaction Mass  
777 Spectrometry: Applications in Atmospheric Sciences, *Chem Rev*, 117, 13187-13229, 2017.

778 Yucuis, R. A., Stanier, C. O., and Hornbuckle, K. C.: Cyclic siloxanes in air, including identification of high levels in Chicago  
779 and distinct diurnal variation, *Chemosphere*, 92, 905-910, <https://doi.org/10.1016/j.chemosphere.2013.02.051>, 2013.

780 Zhang, H., Yee, L. D., Lee, B. H., Curtis, M. P., Worton, D. R., Isaacman-VanWertz, G., Offenberg, J. H., Lewandowski, M.,  
781 Kleindienst, T. E., Beaver, M. R., Holder, A. L., Lonneman, W. A., Docherty, K. S., Jaoui, M., Pye, H. O. T., Hu, W., Day, D.  
782 A., Campuzano-Jost, P., Jimenez, J. L., Guo, H., Weber, R. J., de Gouw, J., Koss, A. R., Edgerton, E. S., Brune, W., Mohr, C.,  
783 Lopez-Hilfiker, F. D., Lutz, A., Kreisberg, N. M., Spielman, S. R., Hering, S. V., Wilson, K. R., Thornton, J. A., and Goldstein,  
784 A. H.: Monoterpenes are the largest source of summertime organic aerosol in the southeastern United States, 115, 2038-2043,  
785 10.1073/pnas.1717513115 %J Proceedings of the National Academy of Sciences, 2018.

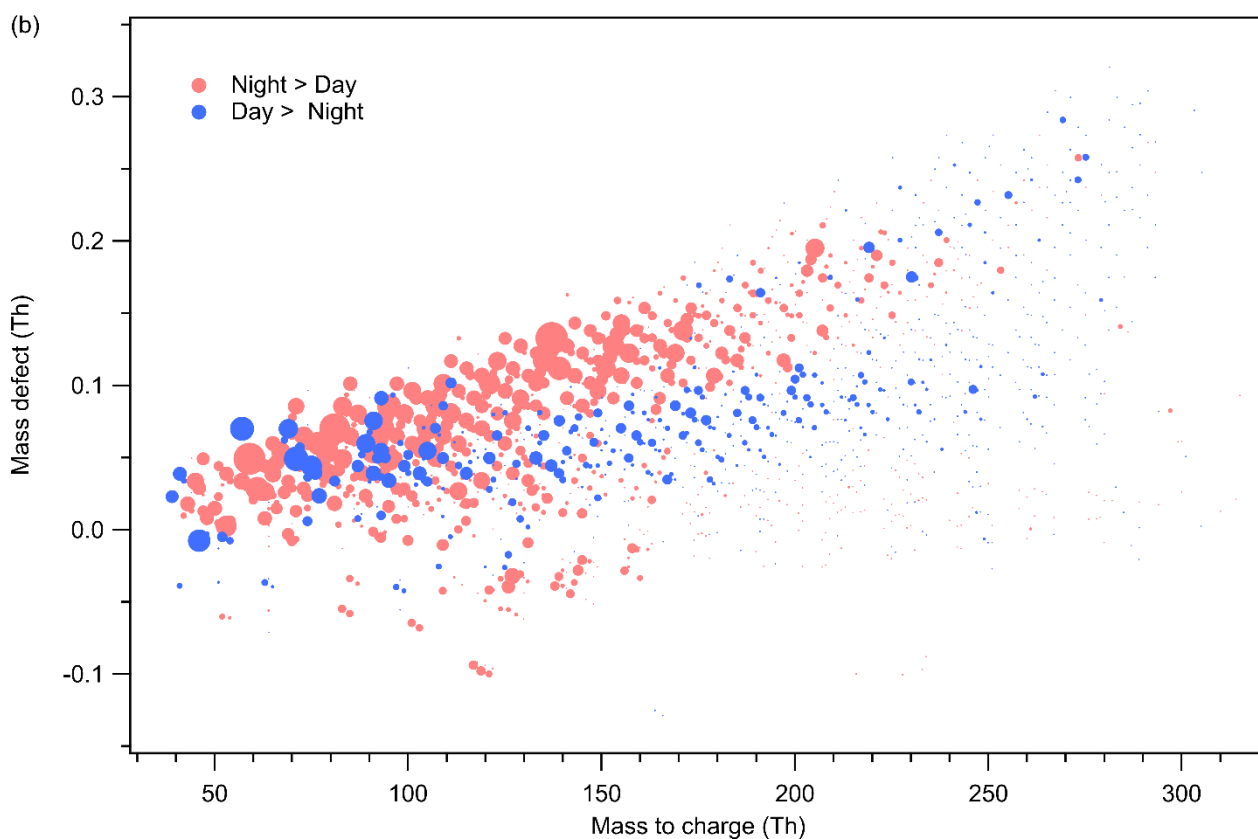
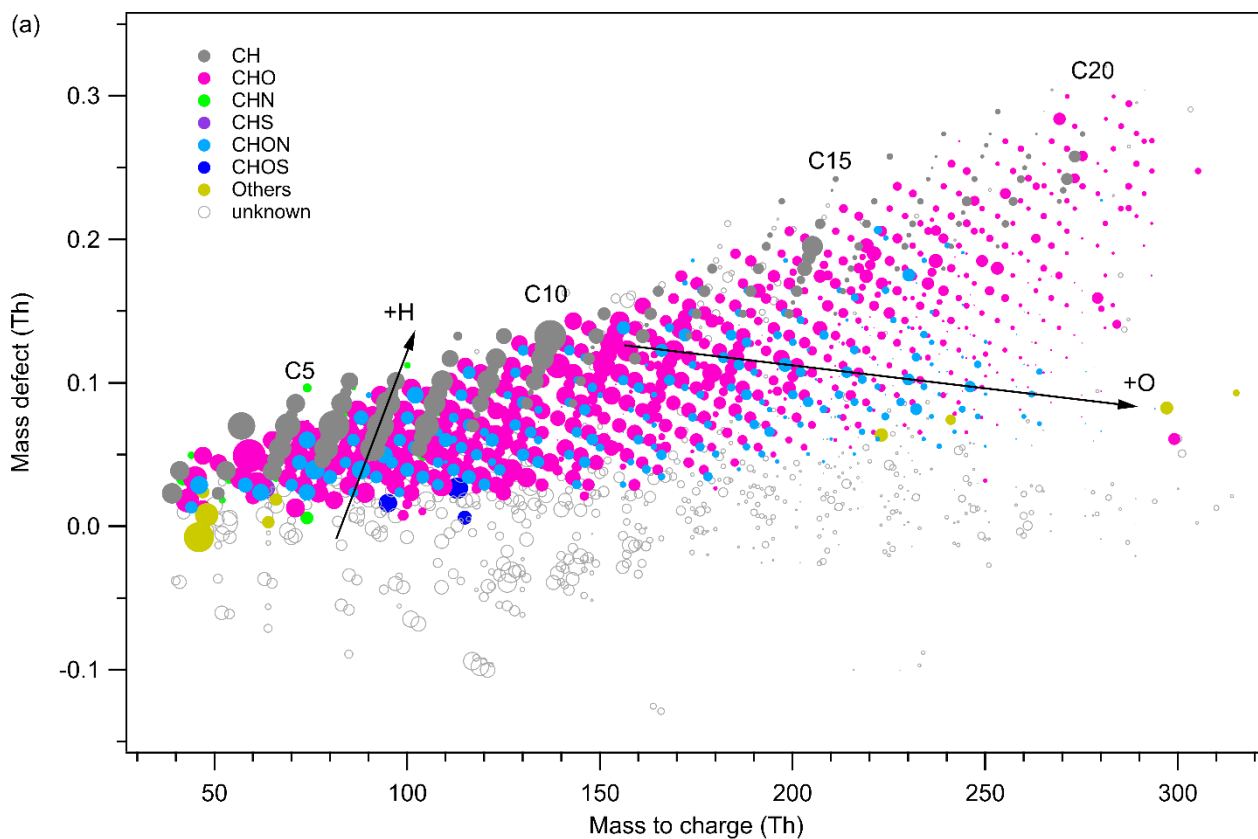
786 Zhu, J., Penner, J. E., Yu, F., Sillman, S., Andreae, M. O., and Coe, H.: Decrease in radiative forcing by organic aerosol  
787 nucleation, climate, and land use change, *Nature Communications*, 10, 423, 10.1038/s41467-019-08407-7, 2019.

788



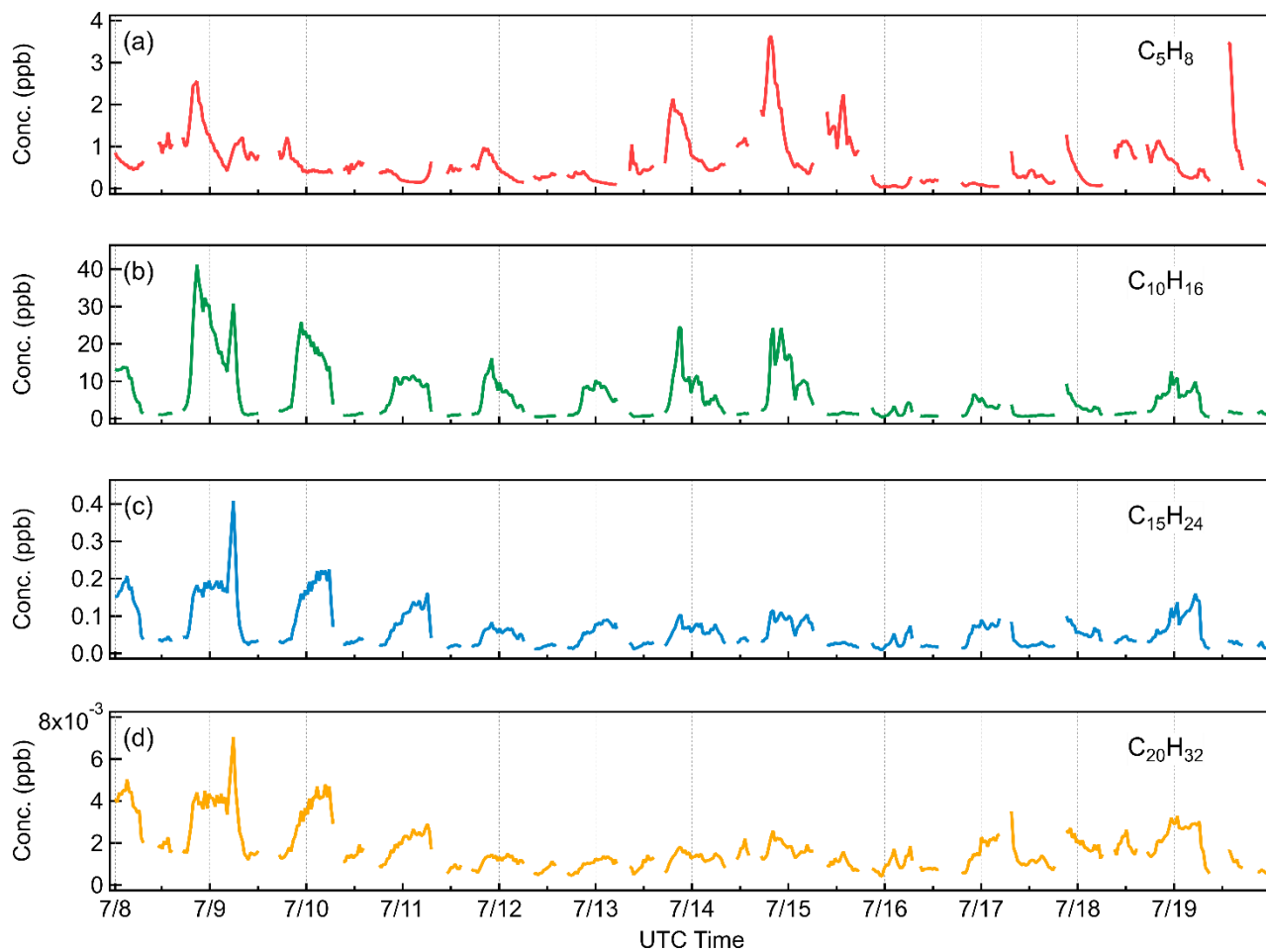
789

790 **Figure 1. Variations of meteorological conditions and trace gases. (a) Time series of wind speed and solar radiation. (b)**  
 791 **Time series of temperature and relative humidity. (c) Time series of  $\text{O}_3$ , NO, and  $\text{NO}_2$ . (d) Diurnal cycles of  $\text{O}_3$  and**  
 792 **solar radiation. (e) Diurnal cycles of NO and  $\text{NO}_2$ .**



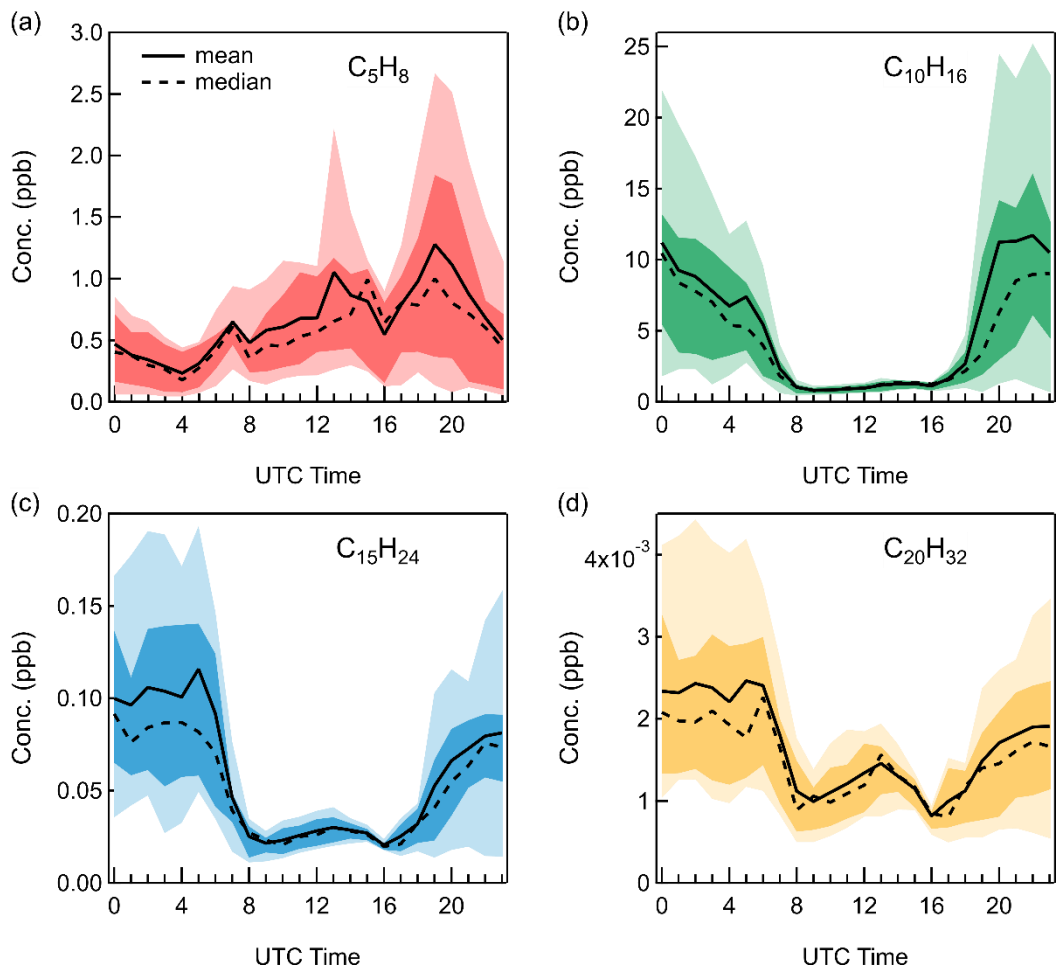
793

794 **Figure 2. Mass defect plot of the ions identified by high-resolution analysis of Vocus PTR-TOF data set. The x-axis**  
 795 **shows the mass to charge ratio and the y-axis shows the mass defect, which is the deviation of the exact mass from the**  
 796 **nominal mass. Data points in (a) are color-coded by ion family (CH, CHO, CHN, CHS, CHON, CHOS) and sized by**  
 797 **the logarithm of peak area. Data points in (b) are shown in pink when signals are higher during nighttime and in blue**  
 798 **when daytime signal is higher. The size corresponds to the difference of daytime and nighttime signal for the molecule.**  
 799 **It should be noted that ions < 35 Th are detected at a much-reduced efficiency due to a high-pass band filter in the BSQ.**



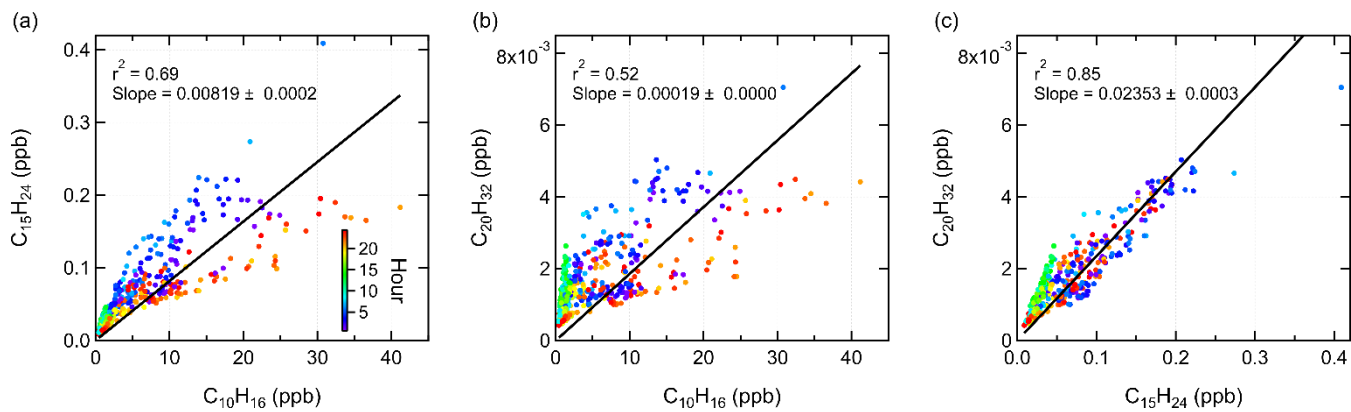
800

801 **Figure 3. Time series of (a)  $C_5H_8$ , (b)  $C_{10}H_{16}$ , (c)  $C_{15}H_{24}$ , and (d)  $C_{20}H_{32}$ .**



802

803 **Figure 4. Diurnal cycles of (a)  $C_5H_8$ , (b)  $C_{10}H_{16}$ , (c)  $C_{15}H_{24}$ , and (d)  $C_{20}H_{32}$ , with the 10<sup>th</sup>, 25<sup>th</sup>, 75<sup>th</sup>, and 90<sup>th</sup> percentiles**  
 804 **shown in the shaded area.**

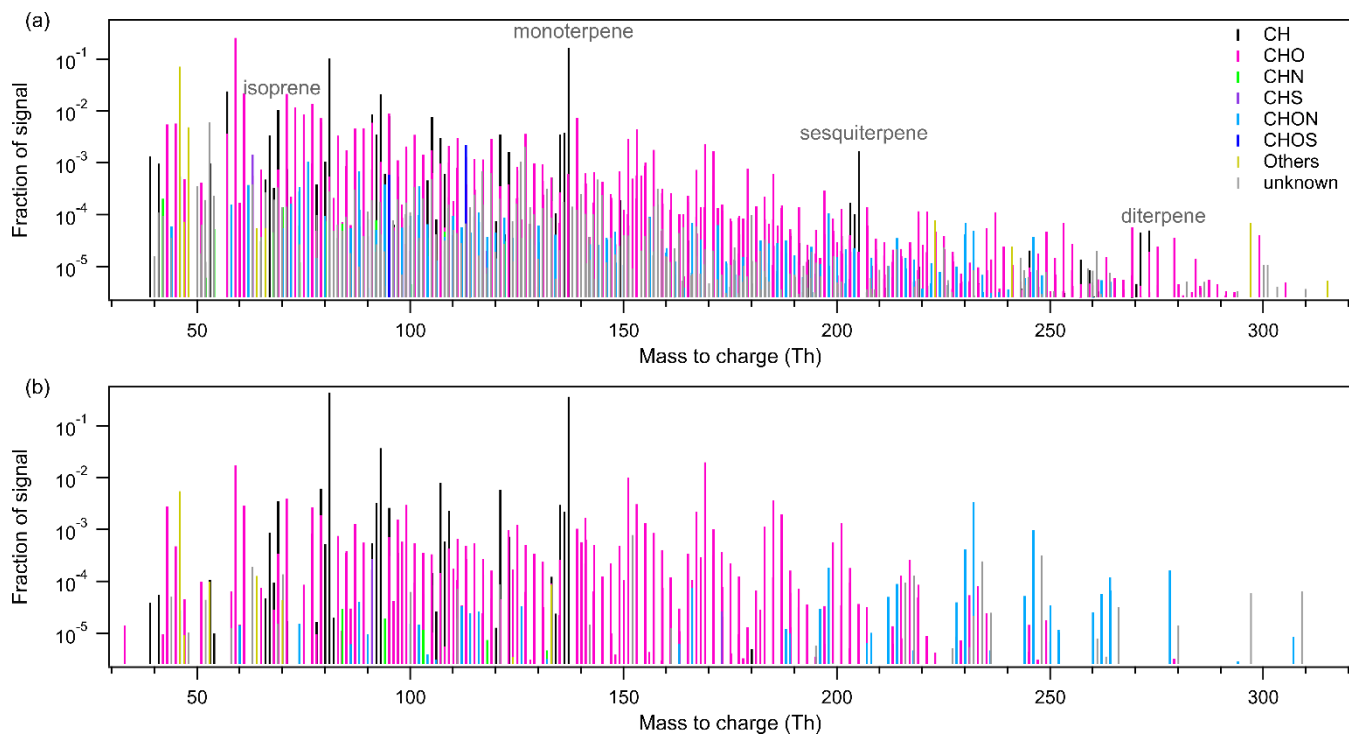


805

806

807

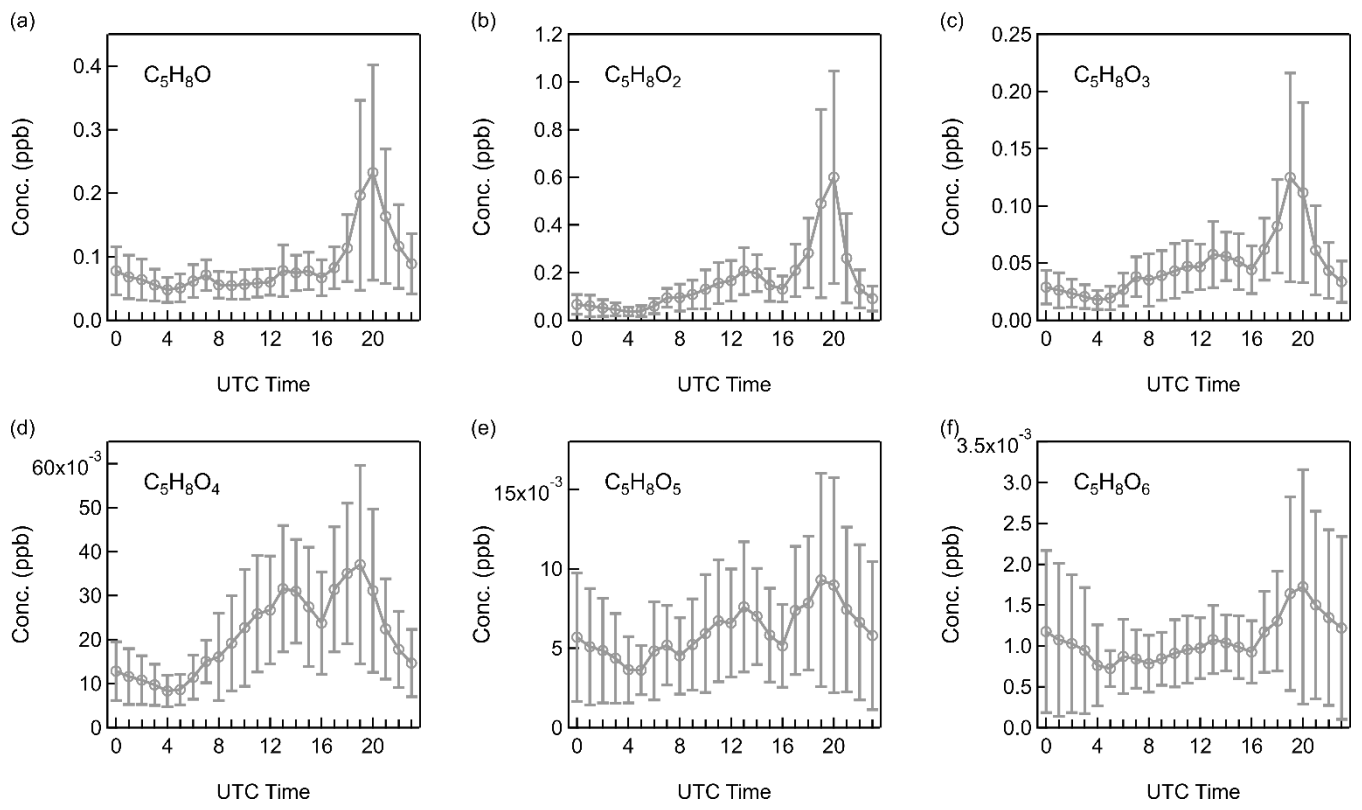
**Figure 5. Scatter plots of (a)  $C_{15}H_{24}$  vs.  $C_{10}H_{16}$ , (b)  $C_{20}H_{32}$  vs.  $C_{10}H_{16}$ , and (c)  $C_{20}H_{32}$  vs.  $C_{15}H_{24}$ , colored by time of the day.**



808

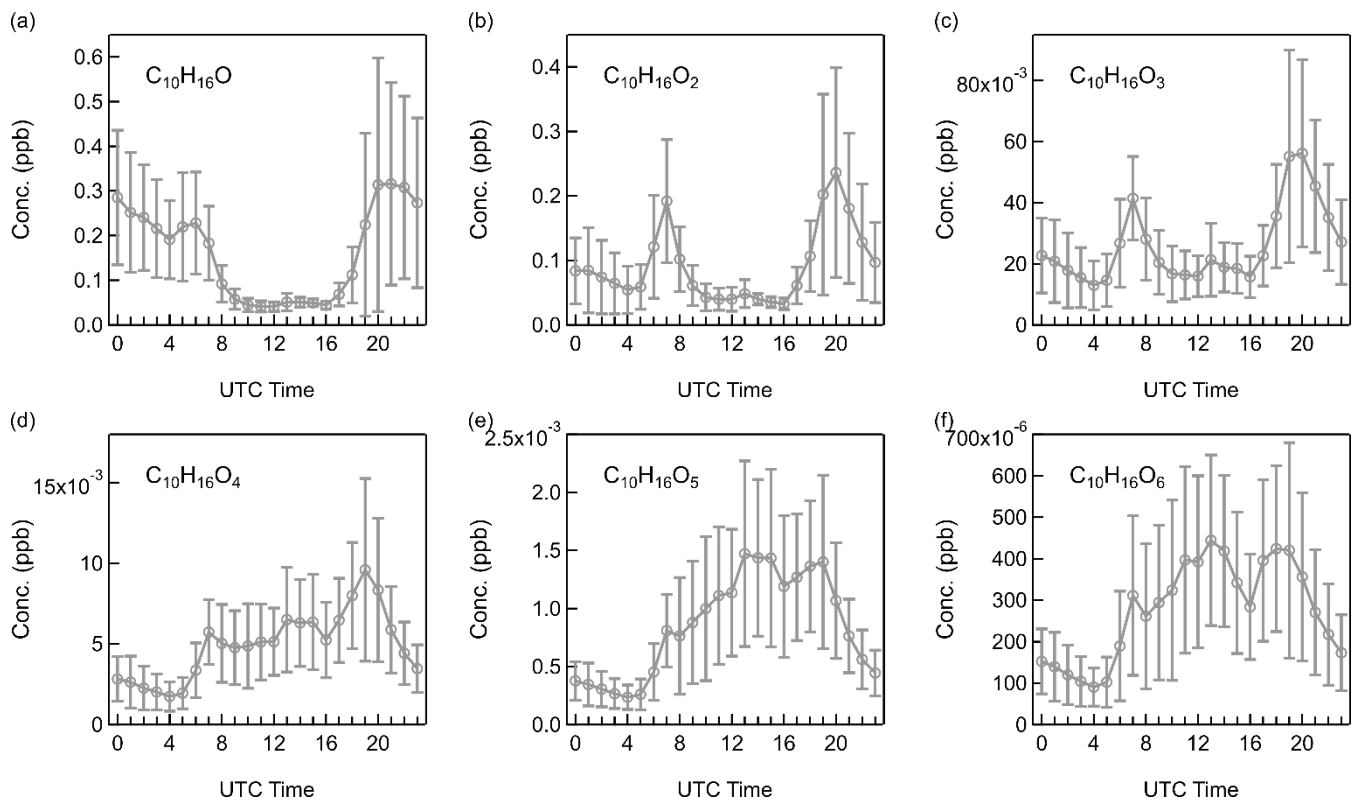
809 **Figure 6. Comparison of ambient average high-resolution mass spectra with those from  $\alpha$ -pinene oxidation experiments**  
 810 **in the COALA chamber. (a) ambient observations in the Landes Forest; (b)  $\alpha$ -pinene ozonolysis with  $\text{NO}_x$ .**





811

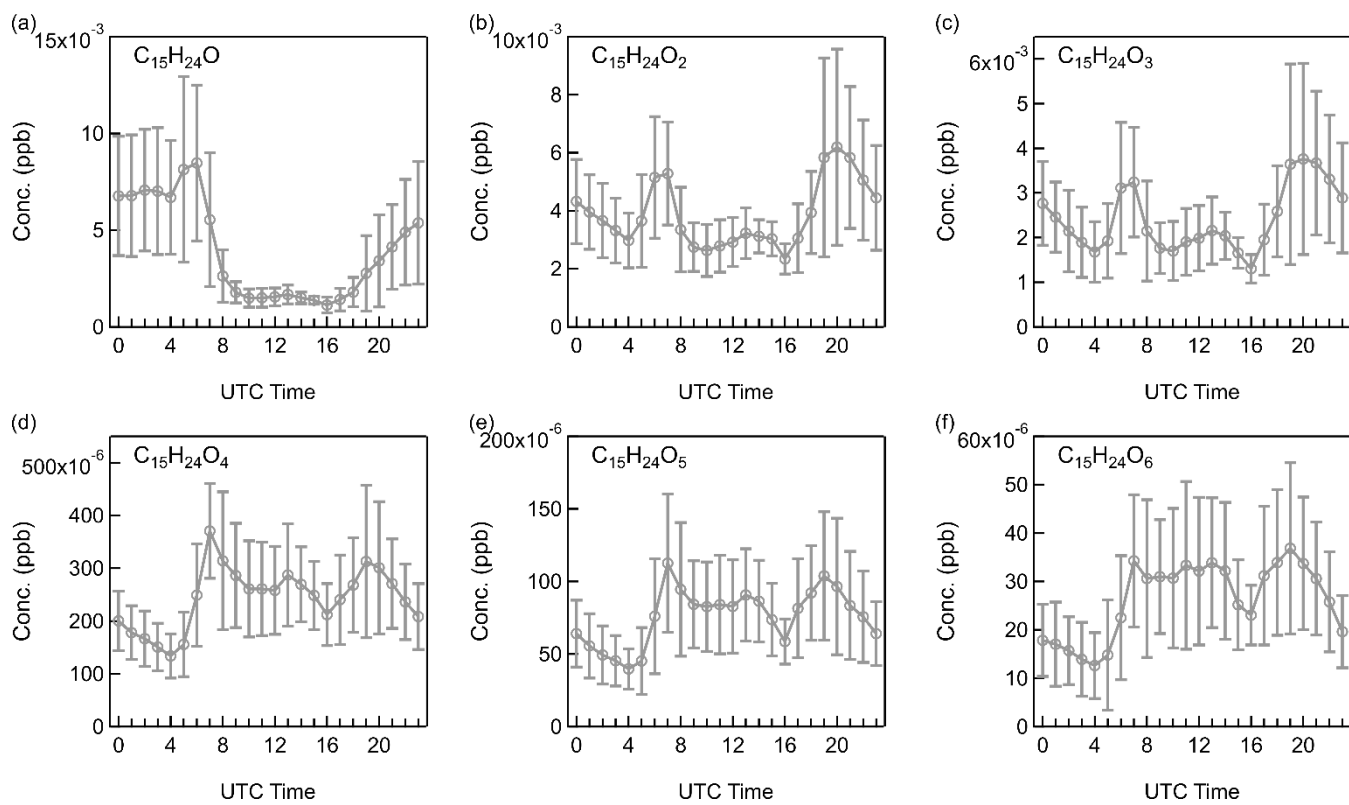
812 **Figure 7. Diurnal patterns of non-nitrate isoprene oxidation products: (a)  $C_5H_8O$ , (b)  $C_5H_8O_2$ , (c)  $C_5H_8O_3$ , (d)  $C_5H_8O_4$ ,**  
 813 **(e)  $C_5H_8O_5$ , and (f)  $C_5H_8O_6$ .**



814

815 **Figure 8. Diurnal patterns of non-nitrate monoterpene oxidation products: (a)  $C_{10}H_{16}O$ , (b)  $C_{10}H_{16}O_2$ , (c)  $C_{10}H_{16}O_3$ , (d)**

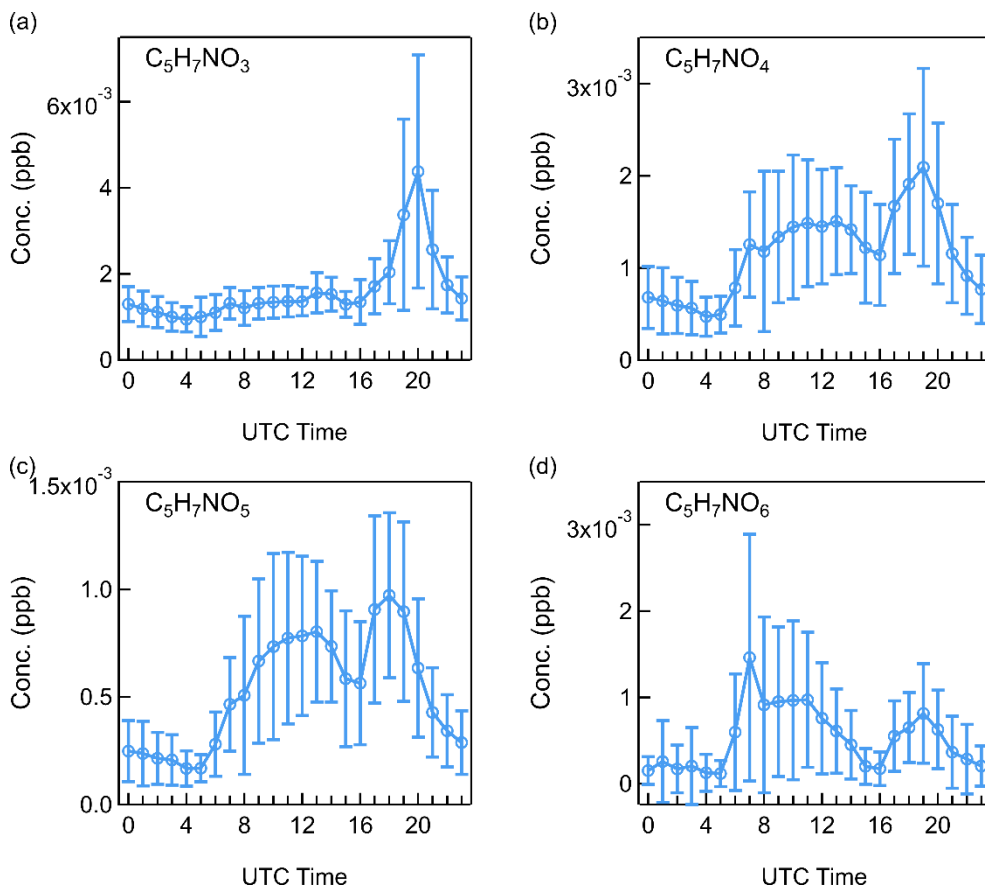
816  **$C_{10}H_{16}O_4$ , (e)  $C_{10}H_{16}O_5$ , and (f)  $C_{10}H_{16}O_6$ .**



817

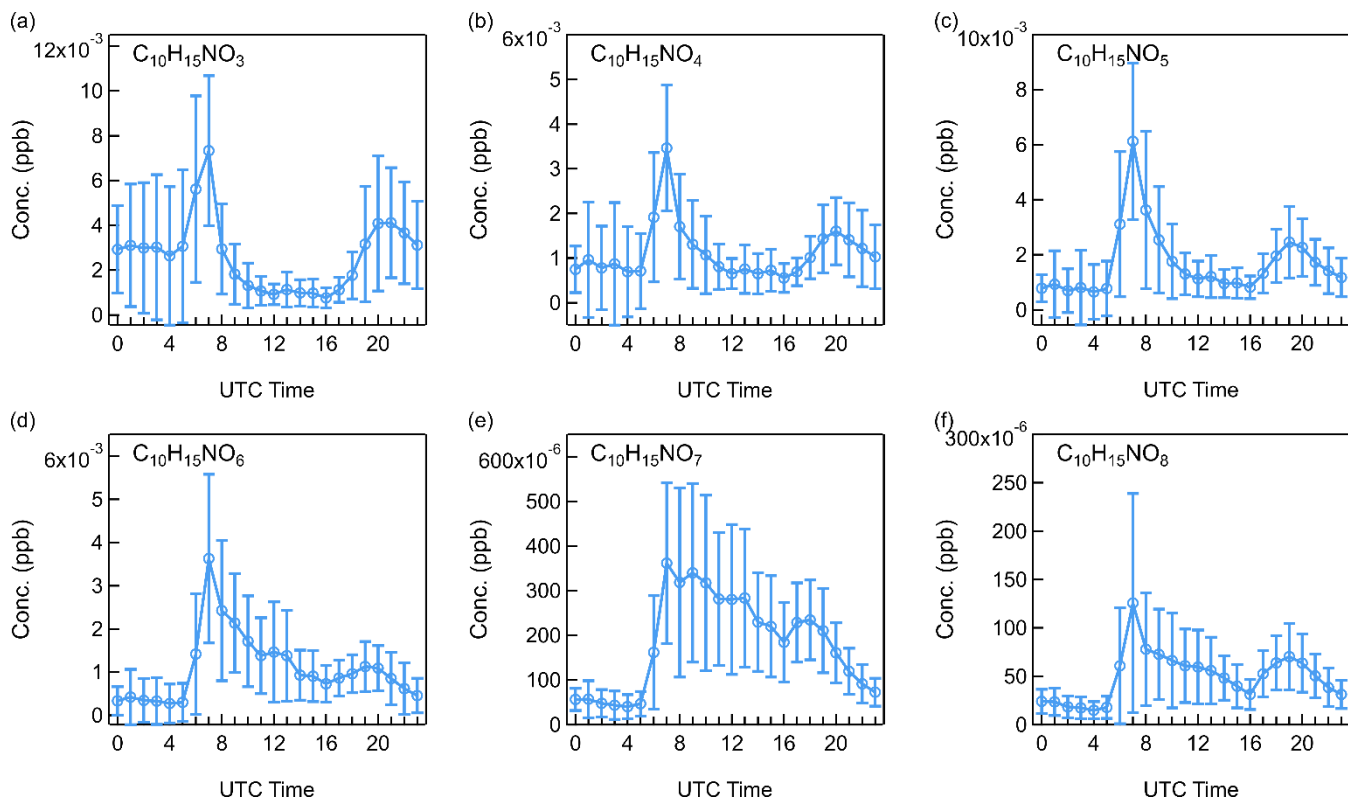
818 **Figure 9. Diurnal patterns of non-nitrate sesquiterpene oxidation products: (a)  $C_{15}H_{24}O$ , (b)  $C_{15}H_{24}O_2$ , (c)  $C_{15}H_{24}O_3$ , (d)**

819  **$C_{15}H_{24}O_4$ , (e)  $C_{15}H_{24}O_5$ , and (f)  $C_{15}H_{24}O_6$ .**



820

821 **Figure 10. Diurnal patterns of isoprene-derived organic nitrates: (a)  $C_5H_7NO_3$ , (b)  $C_5H_7NO_4$ , (c)  $C_5H_7NO_5$ , and (d)**  
 822  **$C_5H_7NO_6$ .**



823

824

825

**Figure 11. Diurnal patterns of monoterpene-derived organic nitrates: (a)  $C_{10}H_{15}NO_3$ , (b)  $C_{10}H_{15}NO_4$ , (c)  $C_{10}H_{15}NO_5$ , (d)  $C_{10}H_{15}NO_6$ , (e)  $C_{10}H_{15}NO_7$ , and (f)  $C_{10}H_{15}NO_8$ .**